

TABLE 1. Revised Photoelectric Photometry for Red Giants in IC 4651

Eggen No.	V	$(b - y)$	m_1	c_1	σ_V	σ_{by}	σ_{m_1}	σ_{c_1}	N_{yb}	N_{uv}
8	10.725	0.678	0.383	0.391	0.000	0.000	0.000	0.000	1	1
22	10.938	0.701	0.420	0.409	0.033	0.007	0.014	0.027	5	5
23	10.645	0.701	0.472	0.273	0.031	0.006	0.015	0.012	6	6
48	12.773	0.793	0.330	0.441	0.026	0.010	0.000	0.062	3	2
58	10.882	0.753	0.481	0.439	0.021	0.004	0.012	0.022	5	5
60	10.852	0.660	0.511	0.454	0.009	0.010	0.000	0.000	1	1
65	10.880	0.758	0.510	0.427	0.003	0.002	0.009	0.016	5	5
76	10.415	0.791	0.573	0.408	0.000	0.000	0.000	0.000	1	1
83	10.933	0.723	0.414	0.402	0.003	0.005	0.008	0.024	4	4
91	10.594	0.654	0.336	0.399	0.015	0.003	0.011	0.020	5	5
93	8.871	1.086	0.767	0.394	0.005	0.005	0.004	0.016	4	4
96	10.358	0.823	0.557	0.439	0.022	0.006	0.010	0.019	4	4
97	11.647	0.820	0.544	0.400	0.010	0.005	0.011	0.032	2	2
98	10.918	0.714	0.457	0.426	0.005	0.002	0.010	0.018	3	3

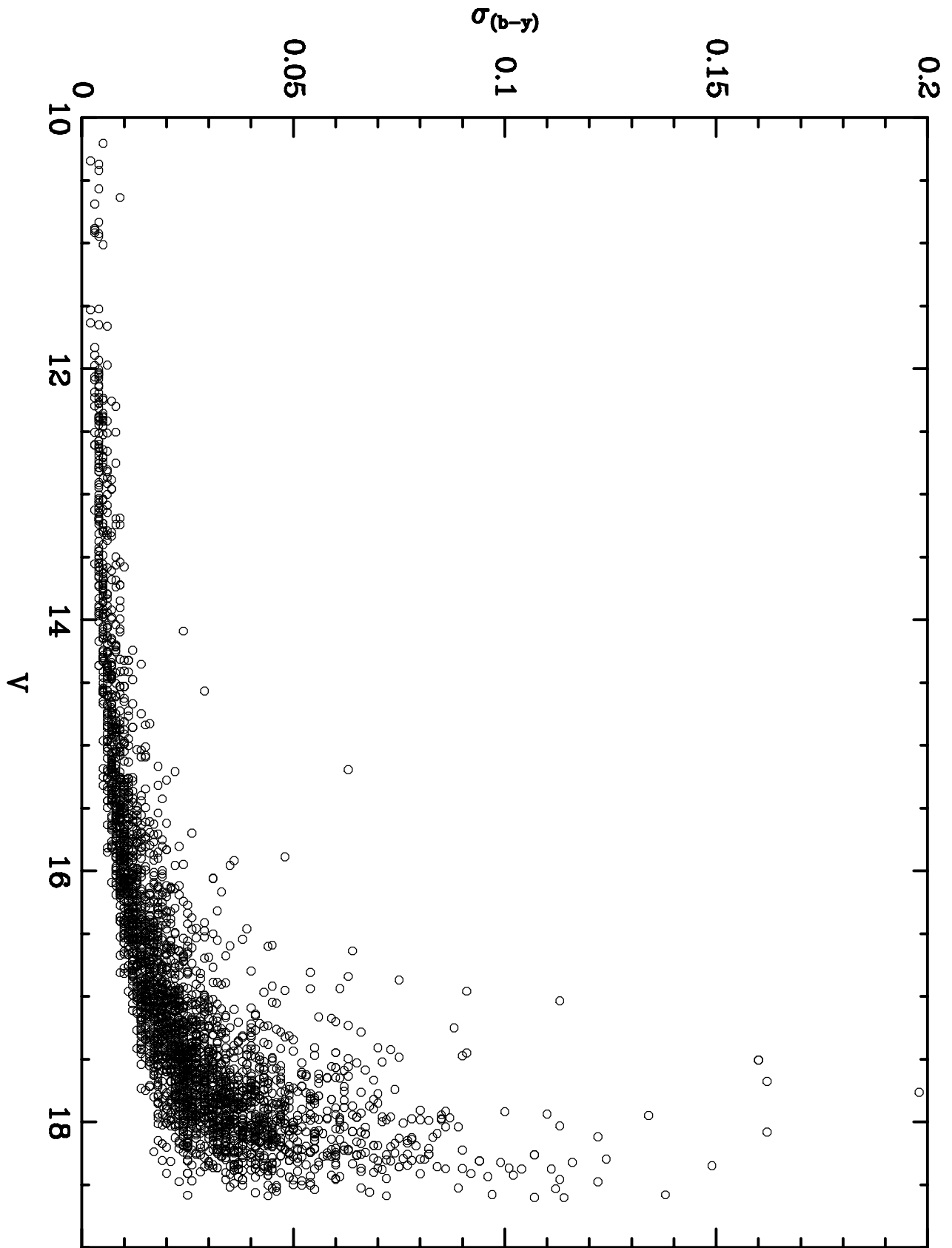


TABLE 2. Summary of Photometric Calibration Equation Coefficients

Star Class	Slope	Color Term	Std. Dev.	No. of Stars
Coefficients for V magnitude				
Blue Dwarfs	1.00	0.03	0.008	10
Cool Dwarfs	1.00	0.03	0.008	10
Red Giants	1.00	-0.02	0.020	9
Coefficients for $(b - y)$ Colors				
Blue Dwarfs	0.959	...	0.004	10
Cool Dwarfs	0.959	...	0.004	10
Red Giants	0.981	...	0.012	9
Coefficients for m_1 Indices				
Blue Dwarfs	1.067	0.11	0.007	4
Cool Dwarfs	1.152	...	0.007	6
Red Giants	1.110	...	0.036	9
Coefficients for c_1 Indices				
Blue Dwarfs	1.016	...	0.003	4
Cool Dwarfs	1.051	...	0.017	6
Red Giants	1.00	...	0.030	9

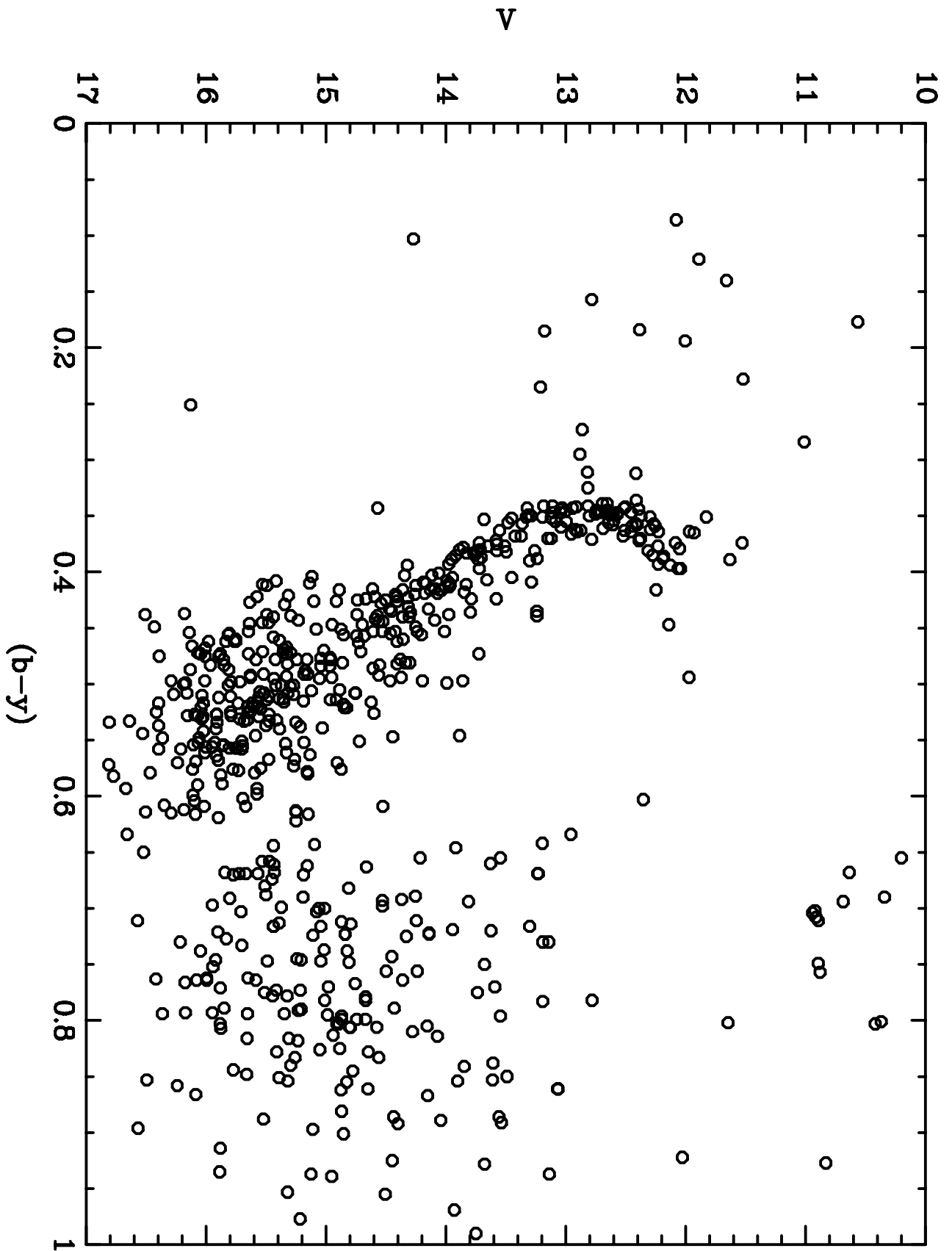


TABLE 3. CCD $uvbyH\beta$ Photometry in IC 4651 ($V \leq 15.0$)

No.	E No.	X	Y	V	$(b-y)$	m_1	c_1	β	σ_v	σ_{by}	σ_{m1}	σ_{c1}	σ_β	$N(y, b, v, u, \beta_w, \beta_n)$
56	93	53.3	53.3	8.899	1.064	0.837	0.317	...	0.004	0.004	0.005	0.003	...	1 4 2 2 0 2
37	27	39.2	-38.2	10.203	0.655	0.349	0.442	...	0.004	0.005	0.007	0.010	...	2 4 2 1 5 7
113	12	-35.7	-53.2	10.344	0.690	0.396	0.437	...	0.002	0.002	0.007	0.009	...	3 5 2 2 5 7
72	96	4.0	69.8	10.371	0.801	0.587	0.390	...	0.003	0.004	0.007	0.009	...	5 6 2 2 6 7
90	76	-64.0	32.0	10.420	0.803	0.593	0.400	...	0.003	0.004	0.008	0.011	...	3 3 2 2 5 7
44	46	43.0	-4.2	10.566	0.177	0.180	0.988	2.883	0.004	0.004	0.005	0.004	0.003	3 4 2 2 5 7
236	91	95.5	73.5	10.574	0.653	0.331	0.450	...	0.004	0.005	0.007	0.007	...	1 2 2 1 0 1
139	23	105.8	-47.2	<i>10.641</i>	<i>0.691</i>	0.51:	0.25:	...	0.005	0.009	0.011	0.011	...	4 4 2 1 - -
419		-56.0	-149.0	<i>10.662</i>	<i>0.938</i>	0.006	0.008	1 1 0 0 - -
122	8	18.7	-102.7	10.688	0.694	0.351	0.422	...	0.003	0.003	0.005	0.004	...	4 3 2 2 5 6
504		-155.1	63.0	<i>10.824</i>	<i>0.956</i>	0.003	0.004	3 2 0 0 - -
97	65	-55.9	1.0	10.881	0.757	0.521	0.405	...	0.002	0.003	0.007	0.010	...	3 5 2 2 5 7
29	60	-10.0	-19.0	10.894	0.711	0.440	0.427	...	0.003	0.003	0.008	0.010	...	4 5 2 2 5 7
27	58	-8.2	-8.4	10.896	0.749	0.496	0.418	...	0.001	0.003	0.006	0.009	...	6 4 2 2 6 7
76	98	-20.2	49.2	10.915	0.708	0.466	0.424	...	0.002	0.003	0.009	0.012	...	3 5 2 2 5 7
146	83	102.1	16.2	10.923	0.702	0.476	0.371	...	0.002	0.004	0.007	0.008	...	6 4 2 2 7 7
137		69.1	-60.0	10.945	0.704	0.412	0.436	...	0.003	0.004	0.006	0.007	...	6 6 2 1 6 6
257		-109.3	113.1	11.012	0.284	0.184	...	2.716	0.004	0.005	0.006	...	0.004	4 3 2 0 5 7
505		-153.8	119.0	<i>11.214</i>	<i>0.836</i>	0.003	0.007	1 1 0 0 - -
222		74.5	-128.1	11.363	0.644	0.342	...	2.527	0.005	0.009	0.012	...	0.007	3 1 2 0 1 1
123		31.7	-93.7	11.523	0.228	0.167	0.856	2.798	0.002	0.004	0.007	0.008	0.002	6 5 2 1 5 7
127		48.3	-90.3	11.530	0.374	0.148	0.530	2.642	0.001	0.002	0.005	0.008	0.002	6 6 2 1 6 7
62	94	38.5	54.2	11.633	0.389	0.162	0.496	2.650	0.002	0.002	0.007	0.009	0.002	6 6 2 2 6 7
75	97	-6.6	47.5	11.648	0.802	0.592	0.336	...	0.003	0.004	0.007	0.009	...	6 6 2 2 6 7
		-171.1	58.8	11.661	0.140	2.819	0.005	0.006	0.002	2 3 0 0 5 5
118		-2.5	-64.1	11.775	0.387	0.164	0.492	2.629	0.006	0.007	0.008	0.007	0.003	1 3 2 2 5 7
12		-25.8	27.9	11.831	0.351	0.150	0.531	2.659	0.002	0.003	0.010	0.014	0.002	6 6 2 2 7 7
153	90	72.1	58.3	11.891	0.121	0.154	1.057	2.906	0.002	0.003	0.006	0.008	0.003	5 6 2 2 7 7
212		2.3	-121.7	11.933	0.365	0.133	0.531	2.669	0.003	0.004	0.007	0.010	0.002	6 6 2 2 5 7
193		-79.4	-30.3	11.971	0.364	0.152	0.503	2.648	0.005	0.006	0.007	0.007	0.001	3 4 2 2 6 7
64	95	27.9	54.5	11.973	0.494	0.209	0.408	2.591	0.002	0.003	0.006	0.008	0.003	6 6 2 2 6 7
92		-72.1	27.3	12.006	0.194	0.225	0.849	2.844	0.003	0.004	0.005	0.010	0.003	4 4 2 1 5 7
138		74.2	-50.2	12.031	0.922	0.662	0.348	...	0.003	0.004	0.005	0.012	...	6 6 2 1 7 7
		82.4	57.4	12.043	0.397	0.158	0.499	2.642	0.004	0.004	0.004	0.001	0.002	3 5 2 2 4 7
199	3	-70.2	-90.2	12.053	0.379	0.173	0.515	2.642	0.004	0.004	0.006	0.007	0.003	2 5 2 2 6 7
14	70	-25.3	11.2	12.065	0.397	0.159	0.493	2.632	0.002	0.003	0.010	0.015	0.004	4 5 2 2 5 7
136		72.2	-70.9	12.081	0.086	0.124	0.957	2.877	0.002	0.004	0.006	0.009	0.003	6 6 2 1 7 7
78		-29.1	37.7	12.087	0.374	0.157	0.515	2.640	0.003	0.003	0.009	0.013	0.002	5 6 2 1 6 7
91	74	-62.8	26.8	12.130	0.394	0.149	0.502	2.628	0.002	0.004	0.008	0.010	0.003	4 4 2 2 5 7
1	54	5.7	4.6	12.142	0.447	0.196	0.347	2.597	0.003	0.004	0.007	0.009	0.002	6 5 2 2 5 7
22	56	0.0	0.1	12.185	0.386	0.161	0.492	2.642	0.002	0.003	0.006	0.008	0.002	6 5 2 2 5 7
36	28	27.0	-33.0	12.192	0.388	0.167	0.476	2.648	0.003	0.004	0.007	0.007	0.003	4 4 2 2 5 7
102		-63.1	-9.2	12.229	0.364	0.155	0.519	2.645	0.003	0.004	0.005	0.008	0.002	4 5 2 1 5 7
2	55	9.5	2.5	12.230	0.393	0.160	0.479	2.651	0.002	0.003	0.006	0.008	0.003	5 6 2 2 5 7
117		-4.5	-46.5	12.233	0.377	0.166	0.501	...	0.004	0.005	0.008	0.011	...	4 4 2 2 0 2
131		46.1	-67.2	12.248	0.416	0.158	0.480	2.631	0.003	0.005	0.007	0.009	0.002	5 6 2 1 5 7
13		-26.7	29.4	12.258	0.359	0.132	0.539	2.654	0.005	0.007	0.013	0.016	0.005	5 6 2 2 7 7
166		20.0	87.2	12.267	0.357	0.165	0.543	2.660	0.004	0.004	0.007	0.009	0.003	5 5 2 2 6 7
194	13	-75.6	-50.1	12.277	0.385	0.148	0.497	2.641	0.004	0.004	0.006	0.007	0.003	3 5 2 2 5 7
11		-23.5	30.8	12.296	0.362	0.152	0.517	2.647	0.002	0.003	0.008	0.011	0.002	6 6 2 2 7 7
		-153.1	109.3	12.298	0.351	2.610	0.007	0.008	0.004	2 2 0 0 5 6
31	39	-20.0	-32.4	12.315	0.381	0.145	0.520	2.637	0.003	0.004	0.009	0.012	0.002	4 6 2 2 5 7
265		-127.9	28.6	12.351	0.348	0.137	...	2.651	0.006	0.007	0.010	...	0.005	1 2 2 0 2 6
187		-84.2	20.5	12.355	0.603	0.228	0.471	...	0.004	0.005	0.007	0.007	...	4 4 2 2 5 7
256		-102.2	110.7	12.376	0.350	0.153	...	2.654	0.004	0.005	0.009	...	0.003	5 5 2 0 5 7
203	16	-43.2	-74.7	12.379	0.370	0.154	0.519	2.660	0.002	0.004	0.005	0.007	0.001	5 5 2 2 5 7
34	40	10.6	-25.5	12.386	0.184	0.217	0.847	2.853	0.004	0.004	0.004	0.004	0.002	3 5 2 2 5 7
93	67	-74.5	8.9	12.390	0.372	0.142	0.520	2.638	0.004	0.005	0.008	0.008	0.003	4 4 2 2 5 7
174	99	-36.0	71.1	12.393	0.344	0.163	0.543	2.661	0.003	0.004	0.010	0.014	0.003	5 4 2 2 5 7
		72.4	59.2	12.407	0.358	0.162	0.493	2.675	0.002	0.004	0.006	0.007	0.003	6 6 2 2 7 6

TABLE 3. (continued)

No.	E No.	X	Y	V	(b - y)	m ₁	c ₁	β	σ _v	σ _{by}	σ _{m1}	σ _{c1}	σ _β	N(y, b, v, u, βw, βn)
168		-15.5	97.8	12.410	0.358	0.151	0.569	2.663	0.003	0.005	0.011	0.013	0.003	5 3 2 2 5 7
261		-136.9	71.7	12.415	0.336	2.652	0.004	0.006	0.003	3 3 0 0 5 7
126		40.7	-80.0	12.416	0.312	0.140	0.634	2.704	0.003	0.004	0.007	0.010	0.004	6 6 2 1 5 7
48	50	45.0	12.1	12.417	0.357	0.166	0.535	2.706	0.003	0.005	0.008	0.010	0.003	5 5 2 2 5 7
23		-14.6	7.0	12.447	0.359	0.148	0.519	2.654	0.002	0.004	0.011	0.014	0.003	6 5 2 2 6 7
157		77.9	79.4	12.455	0.347	0.149	0.548	2.659	0.004	0.005	0.007	0.007	0.004	3 4 2 2 3 5
155		80.4	67.9	12.458	0.364	0.159	0.543	2.659	0.004	0.005	0.008	0.009	0.004	3 4 2 2 4 7
264		-135.9	36.5	12.504	1.485	2.737	0.005	0.008	0.004	2 3 0 0 5 7
107	35	-54.9	-22.5	12.506	0.342	0.153	0.534	2.665	0.002	0.003	0.005	0.007	0.003	5 6 2 2 5 7
190		-96.2	-47.5	12.512	0.363	0.155	0.530	2.653	0.005	0.006	0.009	0.010	0.004	3 4 2 2 5 7
170		-27.7	85.9	12.515	0.343	0.147	0.569	2.656	0.003	0.004	0.011	0.014	0.004	4 5 2 2 5 7
132		51.1	-70.7	12.525	0.368	0.156	0.518	2.656	0.003	0.005	0.006	0.008	0.004	6 6 2 1 5 7
280		-125.7	-57.1	12.542	0.345	0.158	0.520	2.658	0.007	0.010	0.014	0.016	0.004	1 1 2 1 4 7
35		30.0	-22.6	12.572	0.347	0.161	0.513	2.695	0.002	0.004	0.012	0.017	0.007	2 2 2 1 4 1
45	47	46.3	-0.6	12.575	0.349	0.168	0.510	2.723	0.003	0.004	0.007	0.009	0.002	6 5 2 2 5 7
245		-19.3	128.8	12.599	0.775	0.426	0.453	...	0.008	0.011	0.018	0.020	...	1 1 2 2 4 5
24	63	-20.0	-1.5	12.603	0.354	0.147	0.524	2.657	0.002	0.003	0.009	0.013	0.003	5 5 2 2 6 7
364		-78.3	-31.6	12.605	0.349	0.138	0.550	2.661	0.003	0.004	0.006	0.008	0.003	5 6 2 2 6 7
79		-25.4	56.7	12.608	0.358	0.152	0.502	2.666	0.002	0.003	0.008	0.013	0.003	5 6 2 2 6 7
202	17	-46.2	-67.2	12.623	0.348	0.147	0.547	2.663	0.003	0.004	0.006	0.008	0.003	6 5 2 2 5 7
175	100	-42.6	72.3	12.636	0.349	0.157	0.543	2.660	0.003	0.004	0.011	0.015	0.003	5 5 2 2 5 7
42		74.4	-11.6	12.645	0.356	2.730	0.004	0.005	0.003	5 5 0 0 5 7
		-167.4	31.8	12.656	0.339	2.636	0.004	0.006	0.005	3 2 0 0 2 5
142		85.6	-32.8	12.656	0.345	0.166	0.532	2.679	0.003	0.004	0.007	0.011	0.003	6 6 2 1 7 7
269		-155.4	13.9	12.673	0.334	2.650	0.007	0.009	0.004	1 2 0 0 4 5
68		8.4	55.0	12.690	0.361	0.156	0.498	2.658	0.003	0.004	0.006	0.008	0.003	6 6 2 2 6 7
177		-70.9	85.0	12.697	0.339	0.106	...	2.653	0.003	0.005	0.013	...	0.004	4 2 2 0 5 5
272		-127.7	3.1	12.702	0.339	0.147	...	2.661	0.002	0.007	0.012	...	0.005	2 1 2 0 3 7
94	66	-64.9	4.4	12.707	0.347	0.153	0.537	2.664	0.003	0.005	0.009	0.012	0.003	5 5 2 2 5 7
176		-60.8	75.7	12.728	0.346	0.155	0.550	2.658	0.002	0.004	0.008	0.011	0.003	5 6 2 2 5 7
141		98.8	-41.3	12.748	0.345	0.170	0.529	2.662	0.003	0.005	0.010	0.014	0.003	6 5 2 1 6 7
260		-107.4	58.2	12.752	0.348	0.141	0.524	2.658	0.006	0.008	0.013	0.015	0.004	3 3 2 1 5 7
205		-48.4	-80.8	12.756	0.348	0.148	0.520	2.668	0.003	0.004	0.007	0.009	0.004	3 5 2 2 5 7
46	48	56.9	5.7	12.783	0.782	0.318	0.459	...	0.003	0.005	0.009	0.012	...	6 6 2 2 5 7
161	92	50.0	68.3	12.785	0.157	0.146	1.113	2.848	0.003	0.004	0.008	0.010	0.003	6 6 2 2 7 7
115		-16.9	-60.7	12.786	0.371	0.146	0.445	2.646	0.003	0.004	0.009	0.012	0.004	6 6 2 2 5 7
276		-140.0	-41.7	12.787	0.330	2.667	0.008	0.010	0.004	1 2 0 0 3 7
140		105.8	-32.7	12.804	0.350	0.175	0.523	2.663	0.004	0.006	0.010	0.012	0.005	6 5 2 1 6 7
208	5	-23.4	-89.2	12.816	0.341	0.137	0.542	2.680	0.003	0.004	0.006	0.008	0.003	4 6 2 2 5 7
259		-100.7	83.8	12.819	0.325	0.150	0.559	2.660	0.004	0.006	0.010	0.014	0.003	4 5 2 1 5 7
49	72	46.5	23.2	12.820	0.311	0.165	0.641	2.734	0.003	0.004	0.008	0.011	0.002	5 6 2 2 6 7
226		123.3	-16.9	12.830	0.374	0.155	0.458	...	0.007	0.011	0.014	0.013	...	2 1 2 1 0 0
289		-54.0	-135.9	12.866	0.273	2.739	0.005	0.006	0.002	3 3 0 1 5 7
28		-5.2	-16.1	12.876	0.363	0.168	0.453	2.644	0.003	0.005	0.008	0.008	0.006	3 4 2 2 1 2
		-5.1	-46.0	12.884	0.295	0.179	0.769	2.724	0.005	0.007	0.010	0.011	0.014	2 2 2 2 4 1
169		-28.9	95.1	12.906	0.364	0.156	0.469	2.644	0.003	0.004	0.009	0.012	0.003	5 5 2 2 5 7
197	1	-82.7	-79.1	12.915	0.342	0.149	0.530	2.667	0.005	0.006	0.008	0.009	0.003	3 5 2 2 6 6
18	71	-8.7	15.4	12.925	0.362	0.161	0.447	2.652	0.003	0.004	0.009	0.013	0.003	6 5 2 2 6 7
95		-52.2	12.1	12.946	0.343	0.141	0.533	2.660	0.004	0.004	0.009	0.012	0.003	5 6 2 2 5 7
188	68	-80.5	3.6	12.956	0.366	0.147	0.487	2.648	0.004	0.007	0.010	0.011	0.004	5 5 2 2 6 7
		-157.9	36.0	12.960	0.634	2.541	0.005	0.007	0.004	3 3 0 0 5 6
39	26	55.7	-38.2	12.999	0.355	0.158	0.510	2.683	0.003	0.006	0.007	0.004	0.003	6 6 2 2 5 6
104		-72.7	-12.1	13.004	0.346	0.148	0.506	2.661	0.003	0.004	0.009	0.012	0.004	6 6 2 2 5 7
88		-55.2	36.9	13.032	0.343	0.140	0.532	2.673	0.003	0.004	0.009	0.012	0.003	5 5 2 2 6 7
204		-44.6	-79.9	13.042	0.360	0.156	0.495	2.658	0.004	0.005	0.008	0.010	0.004	5 6 2 2 6 7
223		98.9	-72.8	13.043	0.344	0.160	0.515	2.643	0.004	0.005	0.008	0.010	0.004	5 6 2 2 5 7
210		-15.5	-81.7	13.045	0.347	0.104	0.565	2.672	0.003	0.004	0.008	0.013	0.003	5 5 2 1 5 7
121		17.8	-105.4	13.067	0.861	0.758	0.136	2.557	0.002	0.004	0.005	0.011	0.004	6 6 2 2 6 7
147	84	103.1	23.3	13.088	0.355	0.191	0.488	2.670	0.004	0.006	0.008	0.009	0.004	6 6 2 2 6 7
21		-9.1	3.8	13.107	0.347	0.165	0.496	2.666	0.003	0.004	0.010	0.014	0.003	6 6 2 2 7 7

TABLE 3. (continued)

No.	E No.	X	Y	V	(b - y)	m ₁	c ₁	β	σ _v	σ _{by}	σ _{m1}	σ _{c1}	σ _β	N(y, b, v, u, βw, βn)
201	14	-65.7	-58.4	13.112	0.341	0.144	0.510	2.670	0.003	0.004	0.007	0.007	0.004	6 6 2 2 6 7
33	32	2.7	-37.8	13.122	0.352	0.152	0.483	2.656	0.004	0.005	0.009	0.010	0.006	3 5 2 2 2 6
98	61	-43.1	-3.3	13.125	0.370	0.152	0.460	2.648	0.002	0.003	0.006	0.010	0.003	6 6 2 2 6 6
59		35.4	32.0	13.139	0.937	0.790	0.202	2.569	0.003	0.004	0.007	0.019	0.003	6 6 2 2 6 7
		-130.8	91.9	13.143	0.730	0.510	...	2.535	0.005	0.006	0.007	...	0.005	4 6 2 0 6 7
38	41	42.8	-23.2	13.151	0.370	0.158	0.455	2.689	0.003	0.004	0.007	0.008	0.003	5 6 2 2 5 7
106		-62.2	-29.2	13.180	0.185	0.155	1.000	2.906	0.003	0.004	0.007	0.009	0.025	5 6 2 2 6 7
16		-18.3	15.9	13.188	0.341	0.025	...	2.664	0.005	0.009	0.029	...	0.005	2 2 1 0 4 3
		-71.7	84.8	13.194	0.730	2.543	0.006	0.008	0.007	4 4 0 0 4 4
3		9.3	-7.1	13.195	0.783	0.600	0.249	2.552	0.003	0.004	0.008	0.017	0.004	6 6 2 2 7 7
54		58.0	44.1	13.197	0.351	0.152	0.501	2.688	0.003	0.004	0.008	0.011	0.002	6 6 2 2 7 7
105		-65.2	-28.6	13.197	0.642	0.452	0.303	2.550	0.004	0.004	0.006	0.009	0.002	6 6 2 2 5 7
82		-37.8	56.1	13.213	0.235	0.165	0.896	2.811	0.003	0.004	0.009	0.012	0.004	6 6 2 2 6 7
255		-99.1	124.4	13.234	0.669	0.324	0.338	2.533	0.003	0.005	0.009	0.014	0.004	5 5 2 1 5 7
89	73	-55.9	31.2	13.240	0.388	0.162	0.420	2.637	0.003	0.004	0.008	0.012	0.004	5 6 2 2 5 7
		1.0	-139.9	13.243	0.435	0.136	0.524	2.649	0.007	0.009	0.010	0.008	0.003	5 5 2 2 6 6
96		-55.5	9.9	13.262	0.381	0.163	0.421	2.633	0.004	0.005	0.010	0.013	0.004	5 6 2 2 5 7
178		-84.0	84.5	13.289	0.409	0.163	0.438	2.618	0.002	0.005	0.008	0.012	0.003	5 5 2 2 5 7
192		-86.1	-39.7	13.290	0.350	0.144	0.485	2.659	0.004	0.006	0.009	0.009	0.004	5 6 2 2 6 7
134		79.9	-86.9	13.302	0.716	0.547	0.276	2.549	0.003	0.005	0.008	0.014	0.004	6 6 2 1 6 7
286		-87.9	-119.6	13.303	0.390	2.652	0.006	0.007	0.004	3 3 0 1 5 6
61	81	24.7	42.8	13.313	0.349	0.160	0.481	2.675	0.003	0.004	0.008	0.011	0.003	6 6 2 2 6 7
		-126.6	102.1	13.325	0.343	0.141	...	2.633	0.005	0.006	0.008	...	0.004	4 5 2 0 6 7
189		-100.8	-18.8	13.333	0.351	0.160	0.464	2.644	0.004	0.007	0.010	0.010	0.005	4 3 2 2 6 7
214		-11.3	-143.5	13.365	0.357	0.090	0.578	2.664	0.003	0.006	0.013	0.018	0.004	3 5 1 1 5 6
47	49	49.4	7.2	13.373	0.368	0.166	0.441	2.712	0.002	0.004	0.006	0.008	0.004	6 6 2 2 5 7
156		78.6	66.9	13.399	1.192	0.186	0.817	2.645	0.003	0.005	0.013	0.030	0.004	6 6 2 2 6 7
109	34	-49.2	-27.8	13.425	0.368	0.151	0.455	2.648	0.003	0.004	0.007	0.009	0.002	5 6 2 2 6 7
198	2	-79.6	-82.8	13.454	0.352	0.149	0.474	2.670	0.004	0.004	0.008	0.010	0.004	4 6 2 2 6 7
7	53	4.0	14.5	13.454	0.405	0.182	0.370	2.630	0.003	0.004	0.007	0.008	0.004	6 6 2 2 6 7
240		10.1	121.5	13.485	0.356	0.154	0.475	2.668	0.004	0.005	0.010	0.014	0.004	3 4 2 2 4 7
15	62	-31.0	-3.1	13.492	0.850	0.456	0.332	2.517	0.003	0.004	0.007	0.017	0.003	5 6 2 2 6 7
262		-137.5	54.2	13.499	0.382	2.637	0.006	0.008	0.004	4 3 0 0 5 7
200	15	-67.1	-66.1	13.511	0.377	0.150	0.442	2.646	0.003	0.004	0.005	0.005	0.003	6 6 2 2 6 7
274		-134.3	-34.0	13.539	0.891	2.544	0.004	0.009	0.003	2 3 0 0 6 7
8		-1.3	12.3	13.548	0.655	0.697	0.133	2.514	0.002	0.004	0.006	0.014	0.004	6 6 2 2 6 7
		-15.8	-82.5	13.548	0.796	2.530	0.003	0.004	0.005	6 6 0 0 5 6
77		-22.3	34.1	13.553	0.363	0.149	0.470	2.656	0.002	0.003	0.010	0.015	0.003	6 6 2 2 6 7
111		-34.9	-29.9	13.559	0.886	0.540	0.286	2.525	0.003	0.005	0.012	0.019	0.004	5 6 2 2 6 7
162		54.0	92.1	13.564	1.467	2.803	0.005	0.008	0.010	0.011	0.005	6 6 2 2 6 7
		29.2	-22.7	13.577	0.375	0.164	0.441	2.688	0.004	0.010	0.014	0.014	0.008	4 2 2 1 5 3
116	33	-16.7	-46.0	13.577	0.381	0.140	0.469	2.644	0.003	0.004	0.006	0.008	0.003	6 6 2 2 5 7
99	38	-39.2	-11.6	13.581	0.424	0.145	0.550	2.638	0.003	0.004	0.011	0.015	0.003	5 6 2 2 6 7
		-136.1	92.8	13.583	0.372	2.614	0.004	0.006	0.004	4 4 0 0 6 7
67	80	16.1	47.4	13.594	0.770	0.571	0.309	2.544	0.002	0.005	0.007	0.013	0.004	6 6 2 2 6 7
		-157.2	71.4	13.609	0.838	2.538	0.005	0.007	0.005	4 3 0 0 6 7
209		-17.3	-89.5	13.612	0.853	0.688	0.240	2.555	0.004	0.004	0.006	0.020	0.004	6 6 2 2 5 7
172		-47.4	94.5	13.626	0.720	0.419	0.326	2.542	0.004	0.005	0.011	0.017	0.003	5 6 2 2 5 7
254		-88.4	118.8	13.630	0.660	0.369	0.334	2.543	0.004	0.005	0.011	0.018	0.004	5 5 2 2 5 7
50	85	75.4	20.4	13.649	0.377	0.164	0.432	2.689	0.003	0.004	0.005	0.004	0.004	6 6 2 2 7 7
20		-13.1	11.1	13.660	0.407	0.181	0.513	2.659	0.003	0.004	0.011	0.015	0.004	5 6 2 2 7 7
129		46.8	-81.2	13.665	1.075	0.842	0.230	2.537	0.004	0.005	0.009	0.020	0.005	6 6 2 1 7 7
66		18.8	62.5	13.679	0.928	0.630	0.314	2.536	0.003	0.005	0.009	0.016	0.003	6 6 2 2 6 6
271		-139.3	2.1	13.680	0.750	2.538	0.004	0.007	0.004	3 2 0 0 5 7
281		-124.3	-58.3	13.684	0.353	0.179	0.431	2.641	0.006	0.008	0.012	0.012	0.004	2 4 2 2 6 7
206	4	-53.3	-90.9	13.707	0.387	0.140	0.437	2.644	0.003	0.005	0.008	0.009	0.004	5 6 2 2 6 7
112		-23.9	-33.9	13.717	0.380	0.151	0.438	2.634	0.004	0.005	0.011	0.014	0.003	5 6 2 2 5 7
196		-84.2	-73.6	13.720	1.045	0.734	0.290	2.516	0.007	0.009	0.014	0.034	0.005	5 6 2 2 6 7
26	64	-14.3	-2.0	13.723	0.374	0.165	0.418	2.639	0.003	0.004	0.006	0.008	0.003	6 6 2 2 5 7
		-137.9	-88.4	13.723	0.397	2.612	0.009	0.009	0.004	2 2 0 0 5 7

TABLE 3. (continued)

No.	E No.	X	Y	V	(b - y)	m ₁	c ₁	β	σ _v	σ _{by}	σ _{m1}	σ _{c1}	σ _β	N(y, b, v, u, βw, βn)
163		49.6	94.8	13.726	0.473	0.253	0.388	2.606	0.004	0.005	0.011	0.014	0.005	5 6 2 2 4 7
60	82	31.5	41.0	13.733	0.389	0.154	0.425	2.653	0.003	0.004	0.008	0.010	0.004	6 6 2 2 6 7
270		-156.9	5.7	13.738	0.775	2.539	0.005	0.008	0.004	3 3 0 0 5 7
52	86	66.1	33.4	13.744	0.381	0.170	0.413	2.673	0.004	0.005	0.009	0.013	0.004	6 6 2 2 6 7
151		90.1	52.0	13.752	0.990	0.891	0.098	2.551	0.003	0.005	0.022	0.037	0.004	5 6 2 2 6 7
145		97.5	2.9	13.761	0.385	0.152	0.434	2.671	0.003	0.005	0.007	0.009	0.004	6 6 2 2 6 6
135		83.0	-78.5	13.770	0.383	0.161	0.442	2.634	0.003	0.005	0.008	0.012	0.004	6 6 2 1 6 6
179		-86.8	69.3	13.791	0.424	0.199	0.371	2.597	0.005	0.006	0.009	0.014	0.004	5 6 2 2 6 7
		-149.9	91.3	13.797	0.436	2.612	0.004	0.006	0.005	4 4 0 0 6 6
149	87	73.8	36.9	13.813	0.694	0.349	0.344	2.585	0.003	0.005	0.008	0.019	0.003	6 6 2 2 8 7
158		67.0	79.9	13.829	0.383	0.154	0.451	2.642	0.003	0.004	0.007	0.010	0.005	6 6 2 2 4 6
225		126.9	-54.9	13.830	0.767	0.396	0.403	...	0.004	0.010	0.016	0.022	...	2 1 2 1 0 0
191		-89.3	-37.0	13.832	0.411	0.147	0.386	2.605	0.004	0.006	0.010	0.014	0.004	6 6 2 2 7 7
		-146.3	-67.2	13.847	0.418	2.651	0.004	0.009	0.004	2 3 0 0 5 7
110		-60.1	-40.8	13.849	0.841	0.526	0.391	2.531	0.003	0.005	0.009	0.018	0.004	6 6 2 2 6 7
251		-67.6	127.2	13.858	0.378	0.169	0.443	2.621	0.004	0.005	0.008	0.009	0.004	5 5 2 2 5 7
10		-7.6	32.4	13.862	0.497	0.247	0.288	2.584	0.003	0.005	0.013	0.018	0.003	6 6 2 2 7 7
167		5.7	103.7	13.887	0.380	0.165	0.434	2.643	0.003	0.004	0.010	0.017	0.004	6 6 2 2 6 7
195		-83.8	-51.4	13.888	0.546	0.324	0.253	2.526	0.003	0.006	0.010	0.013	0.003	6 6 2 2 6 7
74		-8.0	58.6	13.902	1.103	0.773	0.328	2.528	0.003	0.004	0.010	0.021	0.004	6 6 2 2 6 7
279		-136.9	-51.2	13.904	0.854	2.550	0.004	0.009	0.005	2 3 0 0 5 7
32		-5.2	-33.3	13.918	0.385	0.158	0.405	2.634	0.004	0.005	0.008	0.010	0.005	3 3 2 2 5 5
70		8.3	57.8	13.920	0.646	0.346	0.318	2.552	0.004	0.007	0.014	0.024	0.004	6 6 2 2 7 7
4	57	16.8	-9.5	13.933	0.969	0.801	0.156	2.549	0.003	0.004	0.010	0.022	0.004	6 6 2 2 6 7
150		94.9	44.5	13.938	1.011	0.763	0.345	2.535	0.004	0.006	0.010	0.035	0.004	4 6 2 2 6 7
25		-17.9	1.0	13.946	0.719	0.403	0.344	2.524	0.003	0.005	0.008	0.015	0.005	6 6 2 2 6 7
119	29	14.8	-51.4	13.948	0.405	0.145	0.390	2.619	0.003	0.004	0.010	0.014	0.004	6 6 2 2 6 7
181		-66.1	62.2	13.955	0.389	0.155	0.435	2.633	0.003	0.005	0.010	0.014	0.003	5 5 2 2 6 7
80		-35.8	59.5	13.966	0.411	0.184	0.389	2.617	0.003	0.004	0.011	0.016	0.004	6 6 2 2 5 7
218		47.0	-123.2	13.974	0.413	0.135	0.450	2.630	0.004	0.005	0.009	0.012	0.005	6 4 2 1 6 7
159		62.9	72.5	13.977	0.438	0.197	0.364	2.613	0.003	0.005	0.008	0.010	0.004	6 6 2 2 7 7
266		-149.2	26.8	13.979	0.393	2.610	0.004	0.007	0.005	4 3 0 0 6 7
273		-133.3	-28.9	13.993	0.408	2.609	0.004	0.009	0.004	4 3 0 0 6 7
234		121.7	51.2	13.994	0.499	0.196	0.249	...	0.005	0.007	0.011	0.015	...	2 2 2 2 0 0
232		142.8	13.2	14.008	0.499	0.184	0.457	...	0.009	0.012	0.016	0.019	...	1 2 2 2 0 0
58		41.7	45.2	14.013	0.453	0.194	0.345	2.618	0.002	0.004	0.010	0.015	0.003	6 6 2 2 6 7
231		129.2	10.5	14.037	0.416	0.152	0.436	...	0.004	0.008	0.011	0.011	...	2 2 2 2 0 0
40		63.5	-36.5	14.044	0.889	0.813	0.088	2.556	0.005	0.006	0.007	0.019	0.005	6 6 2 1 7 7
87		-49.8	33.4	14.052	0.416	0.117	0.373	2.606	0.004	0.005	0.009	0.012	0.004	6 6 2 2 8 7
19		-9.8	9.2	14.061	0.401	0.170	0.395	2.625	0.004	0.006	0.010	0.012	0.004	6 6 2 2 7 7
114		-28.8	-68.2	14.065	1.144	0.613	0.650	2.547	0.003	0.006	0.011	0.032	0.005	6 6 2 1 6 7
275		-150.4	-34.5	14.071	0.419	2.614	0.005	0.009	0.005	3 3 0 0 5 7
85		-52.0	52.9	14.074	0.814	0.443	0.338	2.547	0.004	0.005	0.010	0.018	0.004	6 6 2 2 6 7
461		-65.6	33.3	14.089	0.549	0.600	0.229	2.531	0.013	0.024	0.032	0.023	0.008	6 6 2 2 7 7
128		53.2	-80.9	14.094	0.443	0.184	0.373	2.607	0.004	0.005	0.010	0.015	0.005	6 6 2 1 6 7
		-18.9	16.1	14.095	0.415	2.608	0.007	0.009	0.010	2 3 0 0 3 3
101		-64.7	-5.1	14.119	0.403	0.152	0.393	2.621	0.003	0.005	0.011	0.018	0.004	6 6 2 2 7 7
		-166.2	123.1	14.124	0.407	2.575	0.008	0.010	0.005	1 2 0 0 2 6
41		67.6	-27.9	14.130	0.416	0.181	0.372	2.657	0.004	0.006	0.009	0.012	0.005	6 6 2 2 7 7
217		48.5	-131.5	14.142	0.722	0.259	0.436	2.532	0.003	0.005	0.008	0.015	0.004	6 6 2 1 6 7
216		34.9	-144.9	14.148	0.433	2.618	0.004	0.007	0.005	3 4 0 0 6 7
30		-18.2	-23.9	14.153	0.867	0.589	0.299	2.525	0.004	0.005	0.016	0.034	0.004	6 6 2 2 7 7
183		-84.8	58.8	14.157	0.805	0.536	0.241	2.542	0.006	0.007	0.010	0.031	0.005	4 6 2 2 6 5
211	7	1.4	-92.8	14.170	0.410	0.162	0.398	2.618	0.003	0.004	0.009	0.012	0.003	6 6 2 2 6 7
248		-32.4	133.1	14.174	0.413	0.166	0.429	...	0.011	0.013	0.017	0.015	...	1 2 2 2 0 0
43		71.7	-3.4	14.179	0.419	0.171	...	2.703	0.006	0.007	0.014	...	0.004	4 4 2 0 6 7
847		-14.0	8.1	14.188	0.409	0.176	0.385	2.624	0.003	0.006	0.012	0.016	0.004	6 6 2 2 7 7
186		-86.1	21.6	14.198	0.497	0.164	0.451	2.600	0.006	0.008	0.011	0.015	0.005	5 5 2 2 7 7
230		119.9	5.7	14.207	0.456	0.159	0.388	...	0.005	0.008	0.012	0.013	...	2 2 2 2 0 0
51		69.2	29.9	14.216	0.655	0.194	0.417	2.577	0.004	0.008	0.011	0.028	0.007	4 4 2 2 2 6

TABLE 3. (continued)

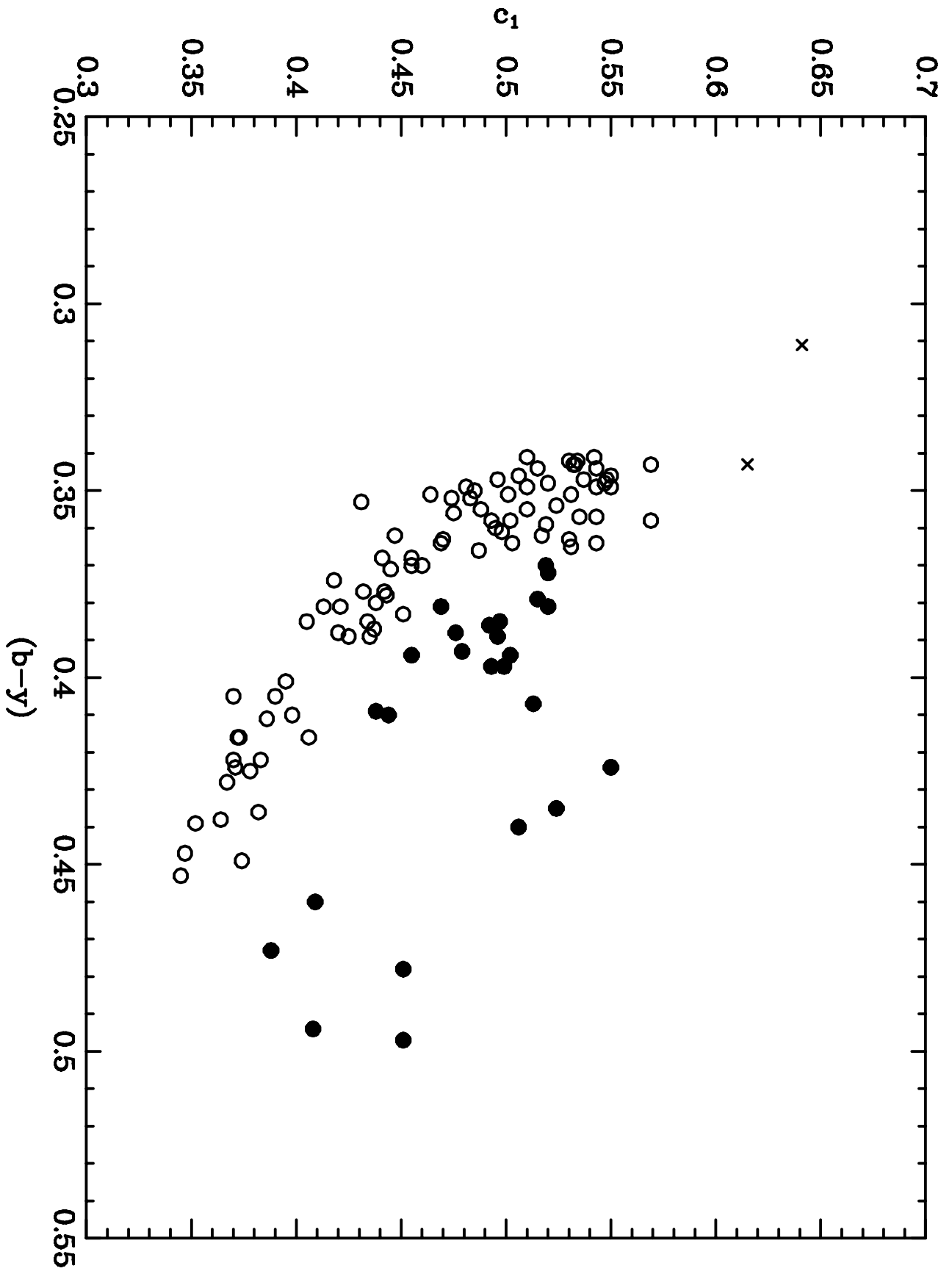
No.	E No.	X	Y	V	(b - y)	m ₁	c ₁	β	σ _v	σ _{by}	σ _{m1}	σ _{c1}	σ _β	N(y, b, v, u, βw, βn)
288		-62.2	-143.8	14.240	0.453	0.054	...	2.606	0.004	0.008	0.020	...	0.004	3 4 1 0 7 7
171		-36.7	88.0	14.241	0.756	0.623	0.241	2.556	0.003	0.005	0.008	0.013	0.005	6 6 2 2 6 7
164		29.6	105.7	14.242	0.399	0.161	0.412	2.643	0.009	0.012	0.016	0.015	0.008	5 5 2 2 5 7
120		15.6	-101.4	14.247	0.711	0.360	0.370	2.512	0.004	0.006	0.009	0.013	0.006	6 6 2 2 6 7
185		-124.0	-86.7	14.254	0.412	2.606	0.007	0.008	0.004	2 4 0 2 6 7
144		91.6	7.2	14.254	0.449	0.199	0.374	2.626	0.004	0.005	0.010	0.012	0.005	6 6 2 2 7 7
258		-118.2	100.3	14.255	0.689	0.189	0.459	2.550	0.005	0.006	0.009	0.019	0.004	6 6 2 1 6 7
124		31.4	-88.7	14.261	0.420	0.185	0.369	2.618	0.004	0.006	0.010	0.014	0.004	6 6 2 1 6 7
267		-145.8	24.2	14.273	0.103	2.631	0.004	0.006	0.011	4 3 0 0 6 7
108		-55.5	-27.3	14.282	0.810	0.545	0.267	2.541	0.003	0.005	0.009	0.019	0.005	6 6 2 2 6 7
215		25.6	-123.8	14.298	0.436	0.163	0.382	2.622	0.004	0.005	0.007	0.010	0.005	6 6 2 2 7 7
		85.1	-24.2	14.303	0.481	0.183	0.350	2.625	0.004	0.005	0.009	0.013	0.005	6 6 2 1 6 7
237		48.8	117.1	14.306	0.440	0.117	0.506	2.621	0.004	0.007	0.012	0.013	0.006	3 3 2 2 3 7
233		112.7	41.5	14.314	0.431	0.151	0.423	...	0.006	0.009	0.011	0.010	...	2 2 2 2 0 0
		121.4	65.4	14.320	0.739	0.372	0.328	...	0.008	0.011	0.013	0.013	...	2 2 2 2 0 0
		-164.9	-44.0	14.321	0.423	2.603	0.008	0.010	0.005	3 3 0 0 5 7
		-140.4	-95.9	14.323	1.074	2.529	0.005	0.011	0.007	3 3 0 0 5 7
		-51.5	-16.8	14.324	0.394	0.160	0.455	2.660	0.004	0.005	0.009	0.011	0.005	6 6 2 2 6 6
		-154.2	-43.8	14.327	0.820	2.554	0.014	0.016	0.008	1 4 0 0 3 4
55		54.1	43.8	14.332	0.725	0.352	0.340	2.576	0.004	0.005	0.011	0.018	0.004	6 6 2 2 7 7
283		-114.5	-68.8	14.339	0.481	2.606	0.005	0.007	0.005	5 6 0 2 6 7
		-132.2	103.1	14.346	0.403	0.185	...	2.597	0.005	0.006	0.008	...	0.004	5 6 2 0 6 7
		-155.4	-77.1	14.353	0.696	2.552	0.013	0.014	0.005	2 3 0 0 5 7
		-100.5	20.5	14.360	0.460	0.204	0.409	2.590	0.004	0.007	0.009	0.010	0.004	6 6 2 2 6 7
253		-74.1	118.3	14.361	0.416	0.172	0.406	2.607	0.005	0.007	0.011	0.013	0.005	5 5 2 2 6 6
		-127.8	99.4	14.363	0.440	0.218	0.369	2.581	0.002	0.004	0.007	0.015	0.005	6 6 2 1 6 7
173		-49.7	94.8	14.364	0.764	0.590	0.253	2.552	0.004	0.006	0.010	0.023	0.004	6 6 2 2 6 7
69		11.3	59.2	14.371	0.692	0.443	0.253	2.576	0.004	0.007	0.010	0.012	0.004	6 6 2 2 6 7
81		-34.3	56.9	14.375	0.494	0.223	0.326	2.591	0.004	0.006	0.014	0.018	0.005	5 6 2 2 5 6
252		-58.3	110.3	14.382	0.478	0.145	0.451	2.597	0.004	0.006	0.009	0.013	0.003	6 6 2 2 6 7
		-134.6	-138.1	14.390	0.413	2.620	0.011	0.014	0.008	1 2 0 0 4 6
130		43.2	-76.2	14.402	0.892	0.727	0.157	2.554	0.004	0.006	0.011	0.023	0.004	6 6 2 1 7 7
83		-32.3	49.2	14.408	0.426	0.184	0.361	2.625	0.003	0.006	0.012	0.017	0.004	6 6 2 2 7 7
224		119.6	-92.5	14.408	0.482	0.178	0.406	...	0.008	0.010	0.013	0.012	...	2 2 2 2 0 0
		-166.9	117.2	14.411	0.462	2.581	0.008	0.009	0.006	3 4 0 0 5 6
148	88	78.2	35.0	14.411	0.422	0.169	0.370	2.648	0.003	0.005	0.009	0.012	0.004	6 6 2 2 8 7
		-164.1	106.1	14.414	0.395	2.582	0.008	0.011	0.006	2 2 0 0 5 6
		-153.4	48.4	14.422	0.420	2.585	0.005	0.008	0.005	4 3 0 0 5 7
		70.4	-24.0	14.425	0.453	0.176	...	2.660	0.005	0.006	0.024	...	0.007	3 3 1 0 2 2
133		59.3	-65.8	14.432	0.789	0.449	0.320	2.552	0.004	0.007	0.014	0.024	0.004	6 6 2 1 7 7
57		44.6	45.1	14.438	0.886	0.556	0.345	2.560	0.005	0.007	0.011	0.022	0.004	6 6 2 2 8 7
810		-3.5	12.3	14.446	0.547	0.243	0.377	2.583	0.005	0.007	0.009	0.015	0.005	3 5 2 2 4 7
		-146.8	104.1	14.450	0.925	2.528	0.005	0.006	0.005	4 4 0 0 7 7
		-156.0	34.0	14.454	0.743	2.557	0.005	0.007	0.006	4 4 0 0 6 6
287		-67.6	-120.1	14.456	0.435	2.620	0.004	0.005	0.004	6 6 0 2 6 7
247		-29.6	124.9	14.464	0.455	0.212	0.432	2.621	0.005	0.007	0.009	0.022	0.005	5 5 2 2 5 7
291		-32.7	-116.6	14.467	0.497	0.171	0.349	2.607	0.004	0.006	0.011	0.014	0.004	6 6 1 2 6 7
		-49.5	-80.4	14.472	0.433	0.194	0.327	2.603	0.006	0.007	0.011	0.019	0.006	6 6 2 2 6 6
278		-143.5	-50.8	14.477	0.800	2.553	0.005	0.012	0.004	3 3 0 0 6 7
63		30.7	61.1	14.501	0.756	0.467	0.275	2.542	0.003	0.005	0.011	0.016	0.005	6 6 2 2 8 6
		104.7	74.9	14.504	0.425	0.165	0.378	2.624	0.004	0.008	0.012	0.012	0.007	4 4 2 2 3 6
819		-64.6	46.0	14.509	0.955	0.808	0.174	2.530	0.004	0.006	0.025	0.041	0.006	6 6 2 1 6 7
		142.6	24.4	14.529	0.444	0.182	0.387	...	0.006	0.010	0.014	0.022	...	2 2 2 2 0 0
		-136.0	-126.6	14.529	0.609	2.593	0.008	0.009	0.006	3 3 0 0 4 6
		-78.4	-135.8	14.532	0.453	2.615	0.006	0.009	0.005	5 4 0 2 6 7
		-133.2	-40.8	14.532	1.059	2.529	0.005	0.009	0.005	4 5 0 0 6 7
		73.7	-134.0	14.533	0.693	0.383	0.389	2.525	0.009	0.009	0.010	0.020	0.007	4 5 2 2 5 7
65		23.3	69.8	14.542	0.428	0.208	0.367	2.621	0.004	0.005	0.006	0.012	0.004	6 6 2 2 8 7
829		-32.5	11.7	14.556	0.483	0.230	0.296	2.582	0.004	0.005	0.017	0.023	0.004	6 6 2 2 7 7
53		51.9	32.9	14.561	0.833	0.494	0.279	2.565	0.004	0.005	0.012	0.019	0.005	6 6 2 2 7 7

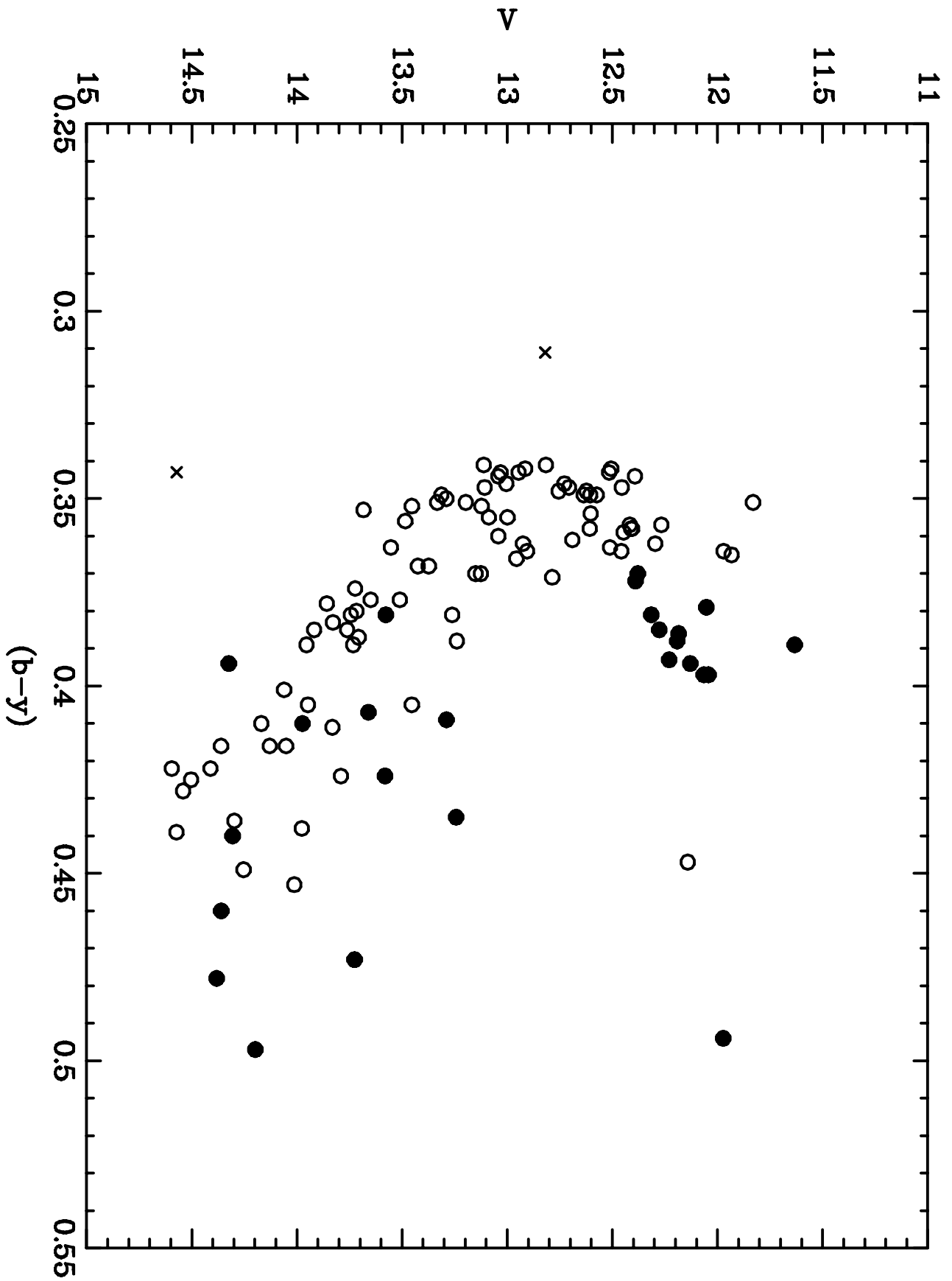
TABLE 3. (continued)

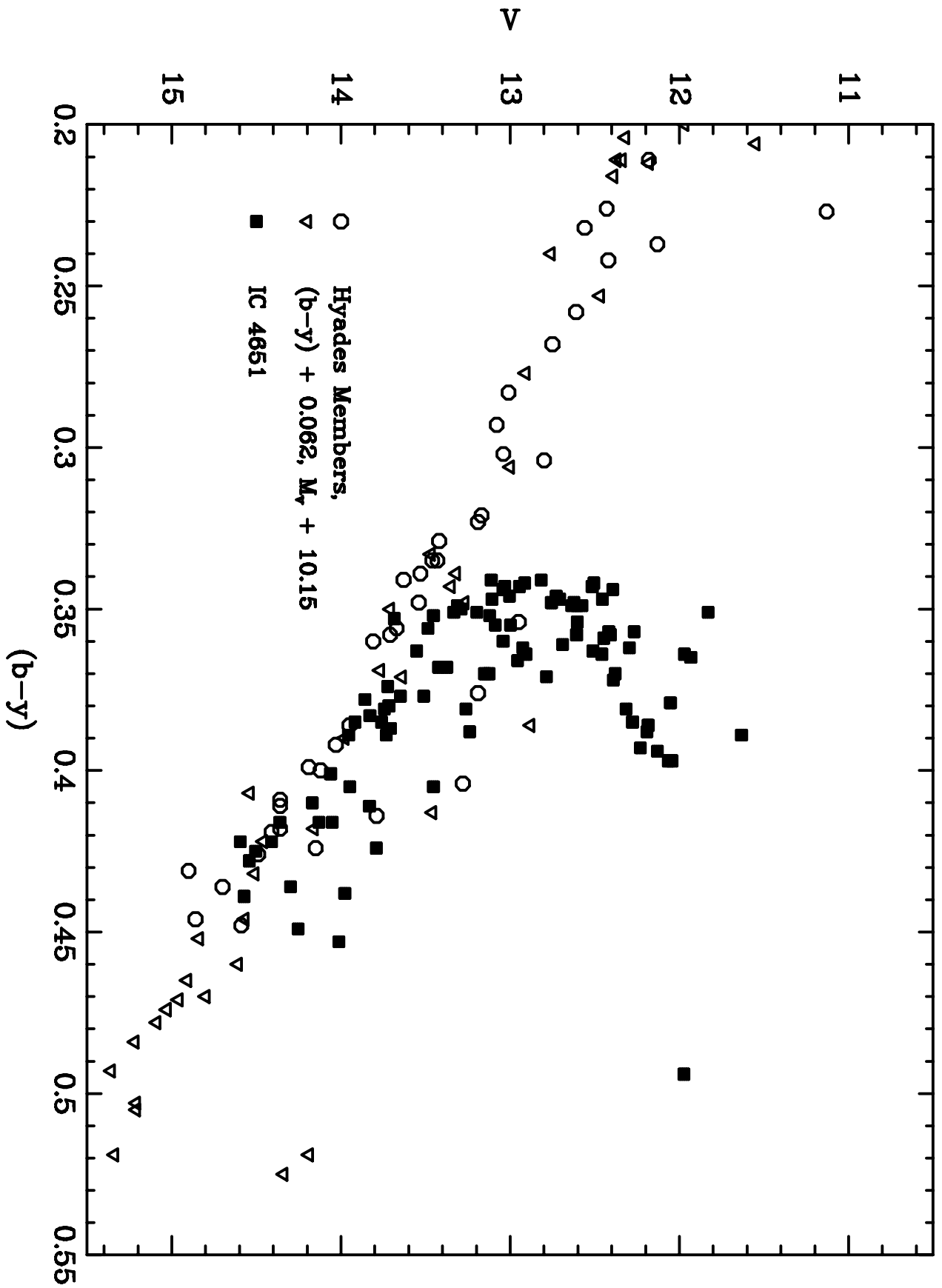
No.	E No.	X	Y	V	(b - y)	m ₁	c ₁	β	σ _v	σ _{by}	σ _{m1}	σ _{c1}	σ _β	N(y, b, v, u, β _w , β _n)
17		-15.1	15.0	14.562	0.444	0.211	0.348	2.597	0.004	0.006	0.018	0.026	0.004	6 6 2 2 8 7
		-79.9	-71.9	14.563	0.492	0.205	0.364	2.606	0.004	0.006	0.009	0.024	0.005	6 6 2 2 6 7
897		-36.6	-50.9	14.565	0.566	0.089	0.474	2.606	0.023	0.029	0.033	0.018	0.015	5 5 2 2 5 7
		-82.5	101.6	14.571	0.343	0.157	0.615	2.692	0.004	0.005	0.007	0.015	0.004	6 6 2 2 6 7
84		-38.6	51.9	14.573	0.439	0.197	0.352	2.610	0.004	0.005	0.009	0.010	0.005	6 6 2 2 6 6
		72.2	51.2	14.580	0.806	0.540	0.283	2.575	0.003	0.005	0.008	0.013	0.004	6 6 2 2 8 7
		-112.3	-130.0	14.591	0.442	2.616	0.004	0.007	0.005	3 3 0 1 5 7
284		-116.2	-74.4	14.593	1.045	2.527	0.006	0.009	0.006	4 6 0 1 6 7
182		-79.3	56.7	14.595	0.422	0.201	0.383	2.607	0.004	0.006	0.008	0.007	0.004	6 6 2 2 6 7
207		-37.0	-100.0	14.601	1.093	0.759	0.283	2.533	0.006	0.008	0.010	0.028	0.005	6 6 2 1 6 7
185		-79.4	28.3	14.603	0.526	0.326	0.259	2.556	0.005	0.006	0.010	0.012	0.004	6 6 2 2 7 7
		-28.7	-92.3	14.609	0.453	0.156	0.390	2.615	0.004	0.006	0.014	0.019	0.005	6 6 2 2 6 7
		56.7	58.9	14.611	0.486	0.239	0.298	2.611	0.006	0.008	0.014	0.017	0.004	6 6 2 2 8 7
184		-89.1	55.5	14.615	0.415	0.163	0.499	2.660	0.005	0.007	0.011	0.012	0.005	5 6 2 2 6 7
		-118.6	-129.9	14.625	0.516	2.587	0.008	0.010	0.006	3 4 0 0 5 7
		128.9	90.4	14.627	0.977	0.824	0.136	...	0.012	0.013	0.016	0.026	...	1 2 2 1 0 0
		62.2	-0.7	14.647	0.828	0.531	0.324	2.620	0.004	0.005	0.008	0.027	0.004	6 6 2 2 7 7
		70.8	114.8	14.651	0.861	0.551	0.318	2.532	0.007	0.010	0.016	0.039	0.010	3 4 2 2 3 5
154		88.3	71.0	14.666	0.663	0.423	0.321	2.562	0.005	0.007	0.010	0.018	0.005	6 6 2 2 5 7
		147.8	-10.2	14.667	0.762	0.362	0.387	...	0.010	0.012	0.014	0.013	...	2 2 2 2 0 0
		80.8	40.7	14.670	0.424	0.151	0.430	2.652	0.003	0.005	0.007	0.010	0.004	6 6 2 2 8 6
		43.8	-131.1	14.671	0.782	0.438	0.288	2.554	0.004	0.007	0.013	0.023	0.007	6 4 1 1 6 7
165		32.4	103.6	14.673	0.799	0.444	0.454	2.572	0.006	0.007	0.015	0.030	0.005	6 6 2 2 6 7
71		2.7	58.6	14.685	0.457	0.178	0.356	2.606	0.005	0.006	0.007	0.009	0.005	6 6 2 2 7 7
		-79.7	83.5	14.698	0.447	0.205	0.390	2.596	0.004	0.007	0.009	0.012	0.006	6 6 2 2 6 7
		39.6	-62.0	14.713	0.471	0.217	...	2.562	0.005	0.007	0.017	...	0.004	5 5 2 0 6 7
		-144.3	-65.9	14.723	0.710	2.525	0.007	0.011	0.006	2 3 0 0 6 7
282		-120.0	-61.8	14.724	0.551	0.682	...	2.583	0.007	0.009	0.110	...	0.005	4 4 2 0 6 7
		-34.8	82.9	14.731	0.463	0.242	0.341	2.582	0.004	0.006	0.015	0.021	0.003	6 6 2 2 6 7
		-153.8	88.1	14.741	0.425	2.578	0.005	0.007	0.004	4 4 0 0 6 6
73		-7.2	74.3	14.744	0.438	0.200	0.355	2.599	0.004	0.006	0.009	0.013	0.005	6 6 2 2 7 7
		-29.7	104.3	14.746	0.799	0.470	0.367	2.544	0.005	0.007	0.020	0.046	0.005	5 6 2 2 6 7
		-161.2	15.5	14.747	0.440	2.581	0.010	0.014	0.008	2 3 0 0 3 6
		-166.3	-6.7	14.747	0.457	2.564	0.005	0.008	0.004	4 4 0 0 6 7
		-102.4	108.7	14.757	0.508	0.296	0.336	2.568	0.005	0.007	0.010	0.022	0.004	6 6 2 2 6 7
		74.0	-77.3	14.760	0.767	0.408	0.351	2.529	0.005	0.006	0.015	0.026	0.004	6 6 2 1 6 7
		113.3	7.1	14.767	0.742	0.378	0.380	...	0.005	0.011	0.015	0.015	...	2 2 2 2 0 0
		19.0	33.3	14.780	0.845	0.483	0.347	2.546	0.004	0.006	0.018	0.028	0.005	6 6 2 2 7 7
		-67.1	112.1	14.795	0.714	0.570	0.257	2.565	0.004	0.007	0.010	0.028	0.004	6 6 2 2 6 7
		62.6	115.0	14.798	0.806	0.502	0.359	2.555	0.004	0.007	0.011	0.040	0.008	4 6 2 2 3 7
290		-33.2	-118.5	14.800	1.288	-0.123	1.175	2.658	0.005	0.008	0.015	0.026	0.006	6 6 1 1 7 7
		-126.9	-53.0	14.804	0.806	0.675	0.126	2.563	0.005	0.009	0.017	0.024	0.005	4 6 2 2 7 7
		43.8	-123.0	14.811	0.748	0.356	0.377	2.542	0.004	0.006	0.010	0.021	0.005	6 5 2 1 6 7
870		11.1	-45.6	14.812	0.579	0.360	0.279	...	0.011	0.013	0.016	0.016	...	1 2 2 2 0 3
		-117.8	-27.7	14.813	0.682	0.487	0.299	2.563	0.005	0.010	0.018	0.025	0.006	6 6 2 2 7 7
		120.0	91.8	14.826	0.738	0.612	0.295	...	0.005	0.008	0.015	0.023	...	2 2 2 2 0 0
		78.6	105.5	14.827	0.760	0.495	0.331	2.556	0.014	0.016	0.026	0.030	0.008	2 3 2 2 2 6
		-67.1	115.5	14.830	0.855	0.696	0.348	2.541	0.005	0.007	0.011	0.021	0.005	6 6 2 2 6 6
		78.7	115.5	14.831	0.521	0.278	0.367	2.576	0.006	0.009	0.019	0.023	0.008	4 3 2 2 3 6
303		-45.8	10.4	14.836	0.485	0.230	0.278	2.577	0.012	0.015	0.021	0.022	0.007	6 6 2 2 7 7
		8.8	-128.8	14.843	0.723	0.367	0.406	2.550	0.004	0.006	0.012	0.033	0.005	6 6 2 2 8 7
		-168.4	72.7	14.849	0.521	2.574	0.006	0.007	0.005	4 4 0 0 7 7
		65.0	89.9	14.855	0.760	0.429	0.403	2.527	0.011	0.012	0.017	0.020	0.009	4 6 2 2 5 7
228		136.7	-17.5	14.856	0.456	0.198	0.362	...	0.004	0.008	0.015	0.018	...	2 2 2 2 0 0
		-91.1	-14.5	14.856	0.518	0.281	0.321	2.573	0.005	0.008	0.012	0.014	0.005	6 6 2 2 7 7
865		-19.6	-50.5	14.856	0.901	0.712	0.167	2.552	0.004	0.006	0.015	0.043	0.005	6 6 2 2 6 7
		121.4	61.9	14.858	0.693	0.290	0.430	...	0.007	0.012	0.016	0.031	...	2 2 2 2 0 0
		8.8	-147.7	14.866	0.481	2.594	0.006	0.008	0.006	4 4 0 0 6 7
		43.8	53.3	14.871	0.881	0.538	0.452	2.555	0.005	0.007	0.011	0.037	0.005	6 6 2 2 8 7
		62.0	-132.4	14.872	0.796	0.620	0.206	2.552	0.007	0.008	0.012	0.019	0.008	5 6 2 2 6 7

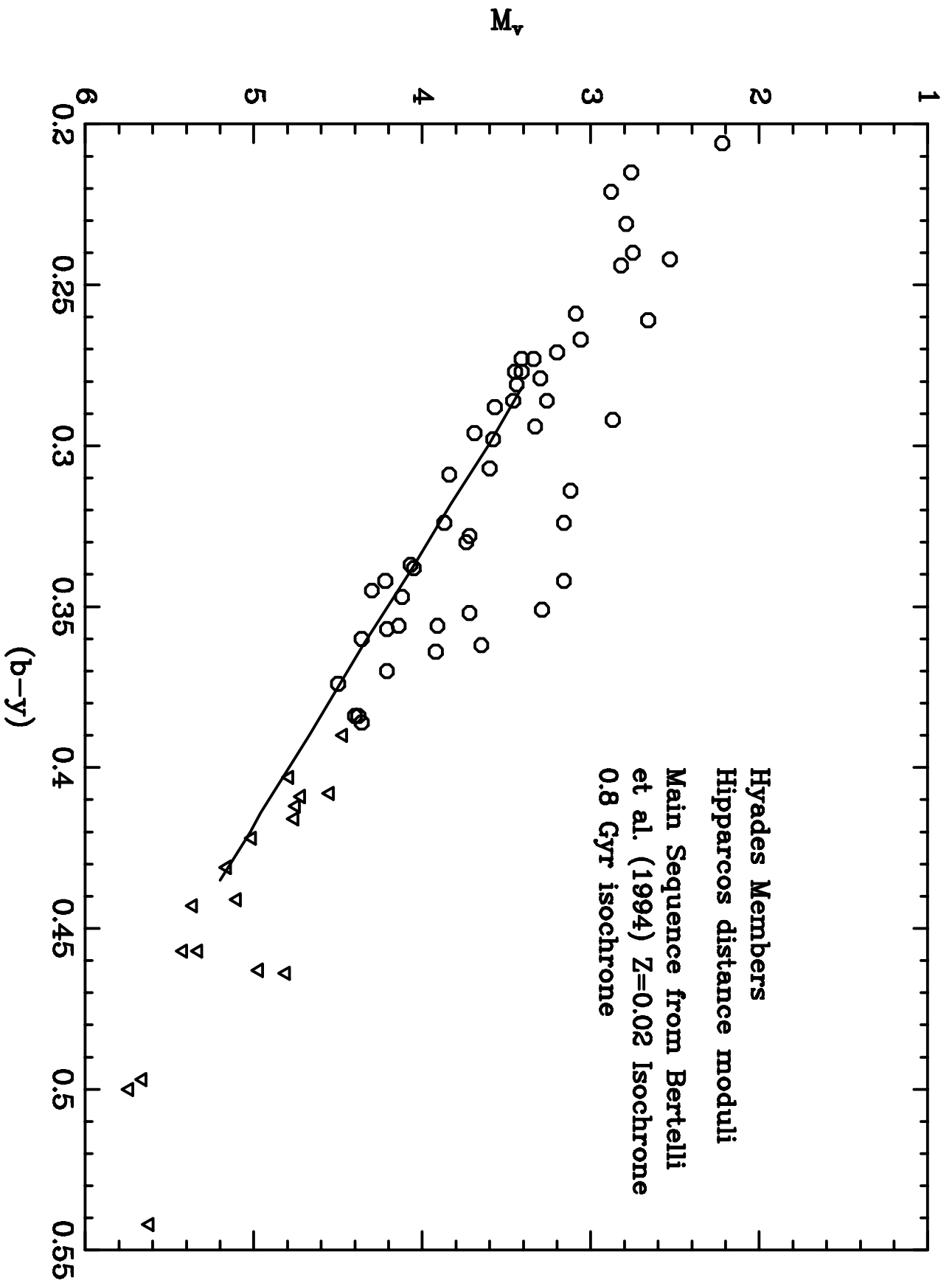
TABLE 3. (continued)

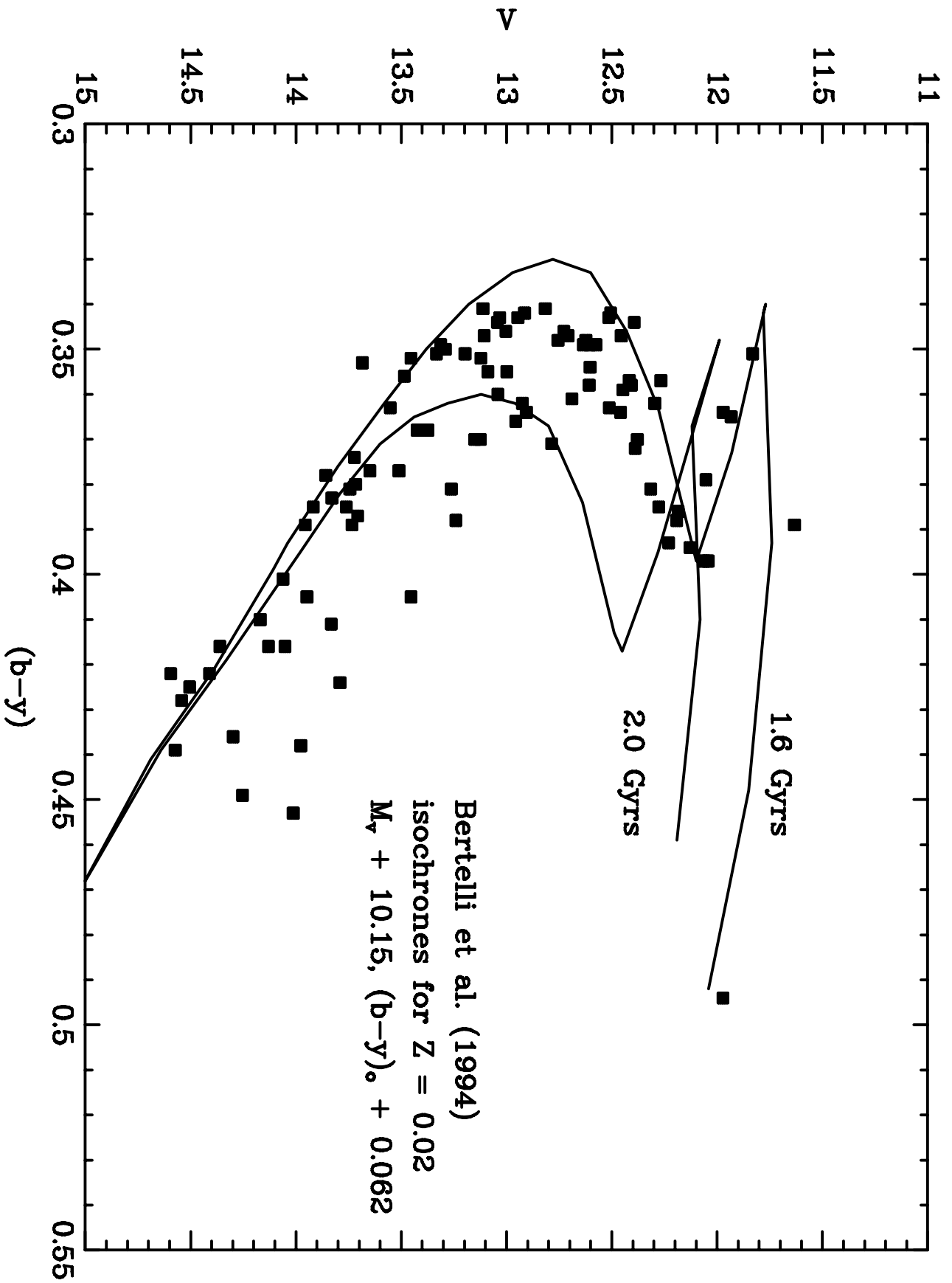
No.	E No.	X	Y	V	(b - y)	m ₁	c ₁	β	σ _v	σ _{by}	σ _{m1}	σ _{c1}	σ _β	N(y, b, v, u, βw, βn)
		109.4	8.8	14.874	0.712	0.268	0.369	...	0.007	0.010	0.014	0.018	...	2 2 2 2 0 1
		-157.2	-82.3	14.875	0.576	2.548	0.007	0.009	0.007	3 3 0 0 5 6
831		-27.0	38.1	14.877	0.862	0.532	0.400	2.528	0.005	0.008	0.015	0.032	0.006	6 6 1 2 8 7
268		-147.9	18.6	14.878	0.451	2.576	0.006	0.009	0.005	4 3 0 0 7 7
100		-40.7	-20.6	14.881	1.265	0.471	...	2.573	0.005	0.007	0.011	...	0.007	6 6 2 0 7 7
		-68.4	51.2	14.887	0.825	0.479	0.352	2.529	0.004	0.007	0.013	0.038	0.005	5 6 2 2 6 7
160		53.8	62.2	14.888	0.505	0.239	0.398	2.615	0.003	0.007	0.009	0.023	0.004	6 6 2 2 8 7
		-173.8	98.0	14.892	0.416	2.574	0.006	0.008	0.007	3 4 0 0 6 5
		-119.2	1.9	14.897	0.803	0.674	-0.060	2.527	0.004	0.008	0.025	0.065	0.006	6 6 1 2 5 7
		40.2	-37.5	14.898	0.357	2.618	0.012	0.020	0.008	2 1 0 0 2 3
		90.1	-52.5	14.906	0.802	0.473	0.357	2.532	0.004	0.006	0.009	0.021	0.005	6 6 2 1 8 7
		-133.2	35.3	14.908	0.570	2.588	0.004	0.010	0.006	4 5 0 0 6 7
		-15.3	80.9	14.913	0.803	0.393	0.387	2.540	0.005	0.007	0.010	0.029	0.007	6 6 2 2 6 7
		61.1	48.4	14.916	0.426	0.178	0.714	2.727	0.006	0.007	0.012	0.016	0.005	6 6 2 2 8 6
		-128.0	-101.4	14.916	0.514	2.594	0.006	0.008	0.005	3 4 0 2 6 7
		-8.2	104.6	14.932	1.014	0.456	0.415	2.542	0.005	0.008	0.013	0.018	0.007	6 6 2 2 6 6
		6.7	113.4	14.942	0.813	0.450	0.374	2.571	0.004	0.007	0.010	0.014	0.005	6 6 2 2 6 7
		-142.6	-59.7	14.946	0.839	2.546	0.007	0.011	0.006	4 3 0 0 6 7
		51.1	85.8	14.952	0.447	0.164	0.437	2.613	0.004	0.006	0.008	0.010	0.005	6 6 2 2 7 7
		56.3	-15.5	14.955	0.494	0.252	0.255	2.661	0.004	0.009	0.013	0.012	0.005	6 6 2 2 7 7
		61.2	-70.8	14.955	0.939	0.845	0.132	2.543	0.004	0.008	0.014	0.028	0.005	6 6 2 1 8 7
		-67.7	-54.3	14.963	0.478	0.205	0.338	2.583	0.004	0.005	0.008	0.017	0.004	6 6 2 2 7 7
		-76.4	-68.7	14.966	0.514	0.190	0.336	2.585	0.004	0.006	0.010	0.013	0.004	6 6 2 2 8 7
		78.3	-112.1	14.970	0.478	0.169	0.348	2.587	0.005	0.006	0.016	0.023	0.006	6 6 2 2 6 7
		123.4	89.1	14.971	0.484	0.209	0.341	...	0.006	0.010	0.020	0.024	...	2 2 2 2 0 0
		-129.6	-91.6	14.982	0.770	2.541	0.008	0.010	0.005	4 6 0 1 6 7
		75.8	-111.1	14.989	0.795	0.517	0.416	2.542	0.008	0.010	0.014	0.024	0.008	6 5 2 1 5 7

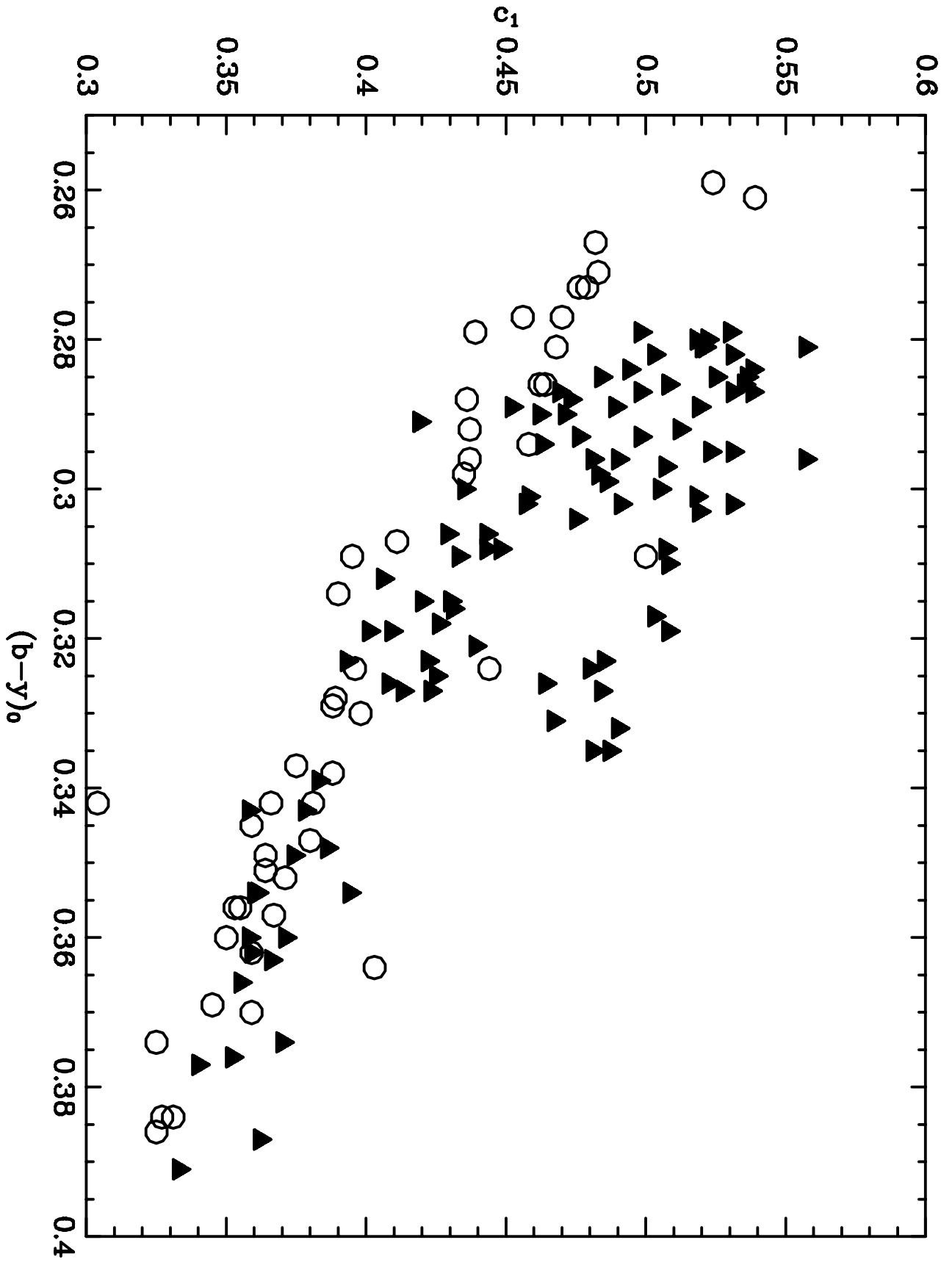


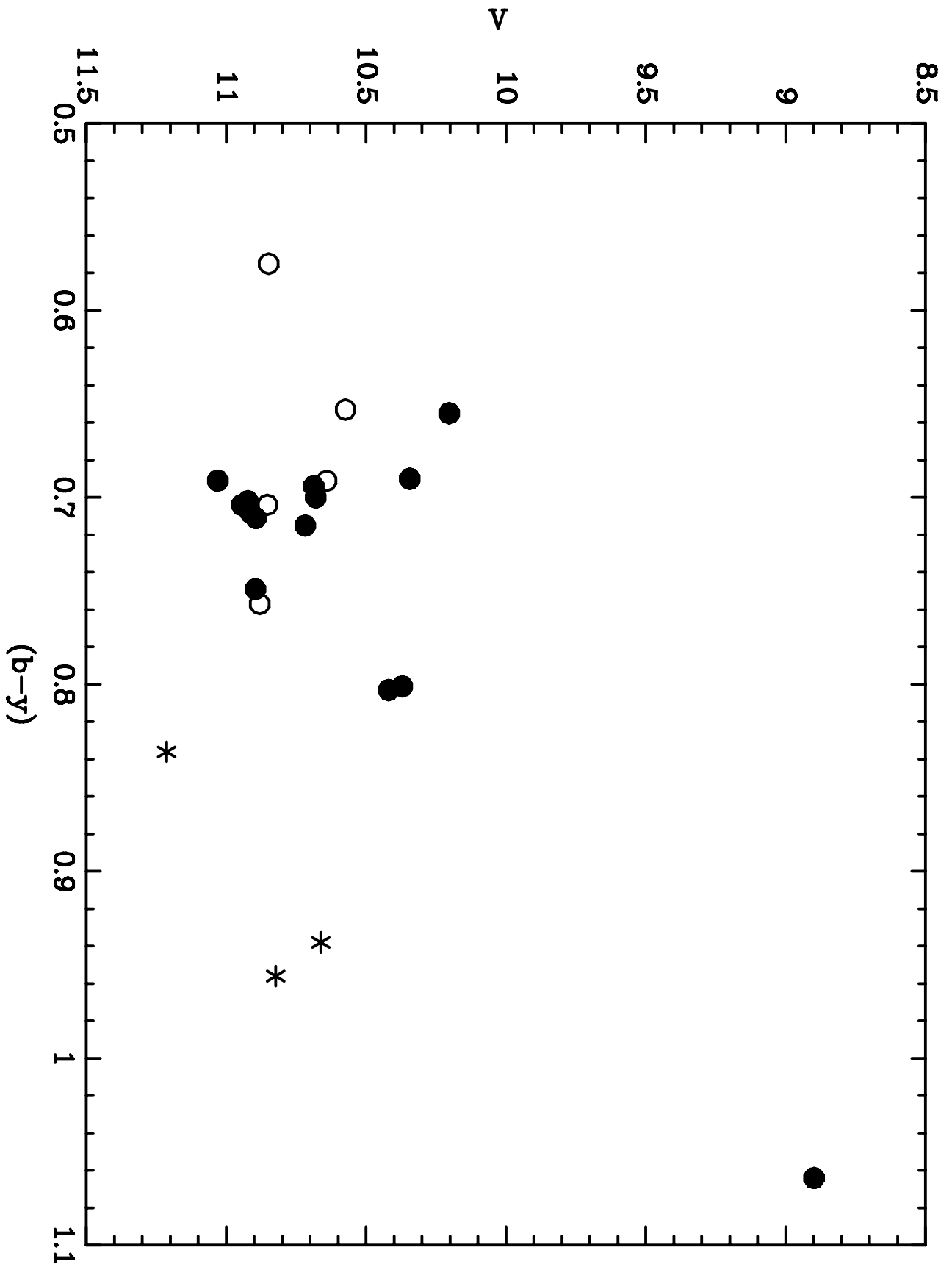


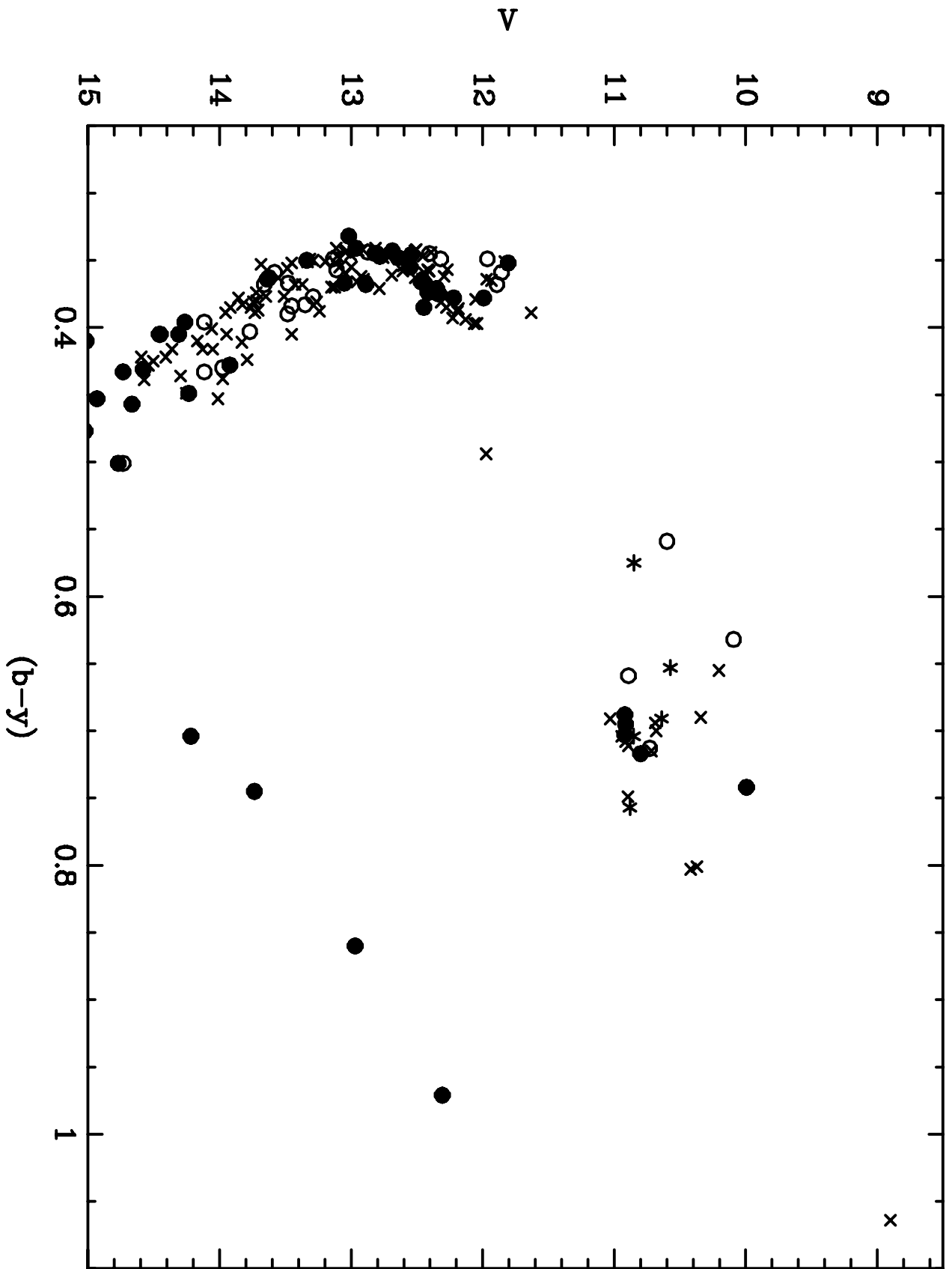












CCD *uvby*H β PHOTOMETRY IN CLUSTERS: I. THE OPEN CLUSTER STANDARD, IC 4651

Barbara J. Anthony-Twarog¹ and Bruce A. Twarog

Department of Physics and Astronomy, University of Kansas, Lawrence, KS 66045-2151

Electronic mail: anthony@kubarb.phsx.ukans.edu, twarog@kustar.phsx.ukans.edu

and

ABSTRACT

CCD photometry of the intermediate-age open cluster, IC 4651, on the *uvby*H β system is presented and analyzed. By using a combination of the information from the color-magnitude diagram (CMD) and the color-color diagrams, a sample of 98 highly probable main sequence cluster members with high photometric accuracy is isolated. From this sample, adopting the intrinsic color relation of Olsen (1988), $E(b - y) = 0.062 \pm 0.003$ and $[\text{Fe}/\text{H}] = +0.077 \pm 0.012$, where the errors quoted are the standard errors of the mean and refer to the internal errors alone. Use of the Nissen (1988) intrinsic color relation produces $E(b - y) = 0.071$ and $[\text{Fe}/\text{H}] = +0.115$. Adopting the lower reddening, a direct main-sequence fit to the Hyades with $(m - M) = 3.33$ leads to $(m - M) = 10.15$, while isochrones with convective overshoot and zeroed to the Hyades produce an age of 1.7 ± 0.1 Gyr, with an excellent match to the morphology of the turnoff. The higher reddening produces $(m - M) = 10.3$ and an age lower by 0.1 Gyr. Comparison with the CMD of NGC 3680 shows that the two clusters have virtually identical morphology which, in combination with their similar compositions, produces identical ages. Coincidentally, the shifts in the CMD necessary to superpose the two clusters require that the apparent moduli of IC 4651 and NGC 3680 be the same, while $E(b - y)_{4651} = E(b - y)_{3680} + 0.04$.

¹Visiting Astronomer, Cerro Tololo InterAmerican Observatory, operated by the Association of Universities for Research in Astronomy, Inc., under contract with the National Science Foundation.

1. INTRODUCTION

In a recent study, Twarog, Ashman, & Anthony-Twarog (1997, hereinafter referred to as TAAT) used a large sample of open clusters to delineate the chemical structure of the galactic disk. TAAT produced a uniquely homogeneous and reliable data set comprising 76 clusters by: (a) eliminating probable non-members and stellar anomalies from the data sample for each cluster; (b) restricting the cluster sample to those with abundances based upon either DDO photometry and/or the moderate dispersion spectroscopy of Friel and her coworkers (see Friel 1995 and references therein); (c) deriving abundances using a revised DDO calibration tied to a large sample of standardized spectroscopic abundances for field stars; and (d) placing the cluster spectroscopic abundances on the same system as the DDO photometry. Surprisingly, analysis of the cluster properties with galactocentric distance, obtained using a common approach for the entire sample, revealed that the clusters with a galactocentric distance less than 10 kpc (on a scale where the sun has $R_{GC} = 8.5$ kpc) exhibited no evidence for a gradient in $[Fe/H]$ with R_{GC} . The cluster abundance distribution had a mean value of solar, with a dispersion of only ± 0.10 dex. A similar result was found for the substantially smaller sample of clusters beyond $R_{GC} = 10$ kpc, with the significant difference that the mean of the abundance distribution was about one-half solar. The implication was that a discontinuity in $[Fe/H]$ occurs at $R_{GC} = 10$ kpc, leading to the conclusion that the chemical history of the disk on either side of this boundary has been different for a large fraction of the life of the disk. Moreover, the homogeneity of the cluster sample on the near side of the transition contradicted the broad range in $[Fe/H]$ found among field stars of a given age (Edvardsson et al. 1993), a result which is interpreted as evidence for stellar orbital diffusion. The field star inhomogeneity occurs because the stellar sample is representative of a broad range in galactocentric distance, including stars formed beyond the discontinuity (see also Wielen et al. 1996).

Although the discontinuous distribution with R_{GC} provided a better statistical match to the abundance gradient than a simple linear fit, within the uncertainty, both were deemed plausible. The greatest source of uncertainty in distinguishing between these two options arose from the rapid decline in the number of clusters in the region of the discontinuity and beyond; 62 clusters are located interior to this point while only 14 are found beyond. We emphasize again, as we did in TAAT, that the discontinuity cannot be the result of a mean age difference between the inner and outer clusters, as suggested by Carraro et al. (1998). The typical interior cluster age lies between 0.0 and 2 Gyrs while the typical anticenter cluster is between 1 and 6 Gyr old. There is no evidence from any study (e.g. Twarog 1980; Carlberg et al. 1985; Meusinger et al. 1991; Edvardsson et al. 1993) for a significant increase in the mean metallicity of the disk in the neighborhood of the sun over the last 5 Gyr. Thus, if we had a sample within R_{GC} of 10 kpc which covered the age range from 2

to 6 Gyr, the mean abundance would be virtually the same as for the younger clusters, a result supported by the handful of clusters in this age range in the TAAT sample. Thus, the discontinuity can be the product of age selection only if the abundance gradient has gotten shallower with time, i.e., the disk beyond the sun has seen a dramatic increase in $[\text{Fe}/\text{H}]$ over the last 5 Gyr while the solar neighborhood has remained constant in $[\text{Fe}/\text{H}]$. This possibility is contradicted by the results of Carraro et al. (1998).

Given the significance of the discontinuity if it is real, a program has been started to improve the data on the sample of clusters in the region of the discontinuity and beyond. By data, we refer to the fundamental parameters of reddening, metallicity, distance, and age. At the time of TAAT, a program was already under way to obtain precise reddening estimates for key clusters using $uvby\text{H}\beta$ CCD observations of stars within the clusters; the program has been modified and expanded to attack both issues. In this paper, we report the first results for IC 4651, a cluster which will be used regularly throughout the program as a link between the instrumental indices and the standard system. In Sec. 2 we discuss the photoelectric $uvby$ data within IC 4651 used to finalize the CCD zero points and their link to the standard system. Sec. 3 discusses the new CCD observations obtained for IC 4651, their reduction, and their transformation to the standard system. The cluster parameters and the color-magnitude diagram (CMD) will be the focus of Sec. 4, while our conclusions are summarized in Sec. 5.

2. PHOTOELECTRIC DATA IN IC 4651 – SETTING THE SCALE

As a test of the robustness of our observational and reduction strategies, IC 4651 will be analyzed as a program object in this paper but, as noted, its continuing role in our observational program is as a secondary calibration object. With this role in mind, the $uvby\text{H}\beta$ photoelectric photometry that exists for cluster stars merits re-examination.

Photoelectric photometry of IC 4651 on the $uvby\text{H}\beta$ system obtained on the 0.9m and 1.5m telescopes at CTIO between 1982 and 1985 was presented in Anthony-Twarog & Twarog (1987); this photometry was then used to calibrate a set of small-format CCD frames to further define the structure of the cluster at faint magnitudes. The photoelectric observations had been transformed to the standard system using the traditional technique of defining nightly calibration curves based upon standard star observations made on each night. The standard system adopted for those transformations was based upon local secondary $uvby$ standards near the South Galactic Pole compiled by Twarog (1984).

However, Kilkenny & Menzies (1986) and Kilkenny & Laing (1992) presented evidence

that the SGP secondary standards did not reproduce the standard *uvby* system as defined by E-region standards for m_1 and c_1 at the 0.01 to 0.02 mag level. Subsequent observations of check stars from the catalog of Olsen (1983) confirmed that the c_1 zero-point for the secondary standards was too large by approximately 0.015 mag. The published photoelectric data for IC 4651 (Anthony-Twarog & Twarog 1987) and M67 (Nissen et al. 1987) include adjustments for this correction. For M67, the c_1 adjustment produced excellent agreement between the independent photometry of Nissen and Twarog, but still a significant offset in IC 4651 remained, with c_1 values larger than those of Nissen (1988) by about 0.025 mag.

The scatter in m_1 was somewhat problematic; no simple offset explained the observed discrepancy with the observations of Kilkenny & Menzies (1986) and Kilkenny & Laing (1992), though there was some indication of a non-linear dependence on $(b - y)$. For M67, the m_1 values of Nissen indicated that those of Twarog were too small by 0.01 mag, the opposite of the effect claimed for the standards, while in IC 4651, no significant offset was found relative to Nissen (1988). Subsequent analysis of the published photometry in M67 by Jøner & Taylor (1997) has demonstrated that the Nissen et al. (1987) data are in excellent agreement with the standard system at a level significantly smaller than the offsets noted above. No additional Strömgen photometry has appeared for IC 4651.

Since the original observations were obtained in the mid-80's the authors have conducted a variety of photoelectric programs involving *uvby* photometry of clusters and field stars independent of the South Galactic Pole program that produced the original secondary standards. Whenever possible additional observations were obtained in an effort to improve the link between the South Galactic Pole data, the secondary standards, and the primary system. With these new observations in hand, the photoelectric data obtained between 1982 and 1986 have been re-reduced. A key alteration from the original procedure is that the photometry is first transformed to a common instrumental system linking, in order, all the observations from different nights of the same run and all the observations from different runs. Once transformed to the common instrumental system, the final transformation to the standard system is made using all appropriate calibration stars observed during the entire program. Details of the procedure may be found in Twarog & Anthony-Twarog (1995).

It should be emphasized that the primary focus of the original program was the hotter dwarfs through mid-G spectral type, so the number of giants observed was small. For this reason, and to avoid nonlinearities often found in transformation equations involving stars of widely differing type, the transformations to the standard system were divided into two color groups separated at $(b - y) = 0.50$. More important, the transformations for the red giants remain tied to primarily the same modest sample observed specifically for IC 4651 as

listed in Anthony-Twarog & Twarog (1987). The revised data for the giants are presented in Table 1.

The final transformation of the program stars, including those in IC 4651, was ultimately tied to 88 *standards* chosen from only two sources, the catalog of primary *uvby* standards as detailed by Perry et al. (1987), and the catalog of field stars by Olsen (1983) transformed to the system of Perry et al. (1987). The dispersion of residuals of the standards about the calibration curves amounted to only ± 0.008 mag for V , m_1 , and c_1 , and ± 0.004 for $(b - y)$.

How do the revised indices for IC 4651 stars compare with the original values that appear in Anthony-Twarog & Twarog (1987)? Red giants excluded, the zero-points of the photometry in V , $(b - y)$, and c_1 remain unchanged with shifts of 0.004 mag or less for each. A change of only 0.001 mag in c_1 confirms the original offset applied to the photometry based upon a much smaller sample of check stars. A change in the m_1 zero-point at the 0.011 level does occur and, in the mean, is in the same sense implied by the standard comparisons of Kilkenny & Menzies (1986) and Kilkenny & Laing (1992) in that the original m_1 indices were too large by between 0.01 and 0.02 mag, on average. Closer examination of the residuals, however, reveals that the offset is not uniform, but is dependent upon m_1 in the sense that larger m_1 values require smaller offsets.

Which system is the *correct* one? As exemplified by the discussion of NGC 752 in Jonev & Taylor (1997), even additional independent observations may not resolve in an internally consistent manner all of the apparent discrepancies among the various systems. Because of the links to the published M67 data (Nissen et al. 1987) and a desire to tie into the cluster photometric system of Nissen (1988), we have chosen to combine the photoelectric photometry of Nissen (1988) and the original photometry of Anthony-Twarog & Twarog (1987) to compare with our CCD photometry; an average of offsets implied by these comparisons will be applied to the calibrated *uvby* indices to force conformity to the composite system.

Since the publication of the original *uvby*H β survey (Anthony-Twarog & Twarog 1987) and the broad-band *BV* survey (Anthony-Twarog et al. 1988), a modest amount of work has been done on IC 4651. The most valuable of the studies is the Geneva photometric and radial-velocity survey of the red giants by Mermilliod et al. (1995). Though the sample includes only giants, 12 stars overlap with the data in Table 1. If star 8 of Eggen (1971; hereinafter referred to as EG) is excluded, the remaining 11 stars exhibit a mean residual in V , in the sense (Table 1 - ME), of $+0.005 \pm 0.019$, confirming that they are on the same system at the ± 0.01 mag level.

In contrast, Piatti et al. (1998) have published a CCD VI survey of 10 open clusters, including IC 4651, to be used as templates for defining CMD morphology with age in VI . Despite claims of accuracy for the brighter stars at the ± 0.02 mag level in V , a simple check with the photoelectric values from Anthony-Twarog & Twarog (1987) for 22 stars in common produces a mean residual in V , in the sense (ATT - PI), of $+0.199 \pm 0.054$. The large scatter is readily explained if the data are divided into southern and northern groups comparable to the probable pair of fields used in the CCD survey. The mean residual for the 11 stars in the southern half is $+0.154 \pm 0.032$, while the northern 11 stars have $\Delta V = +0.245 \pm 0.022$. Such internal and external discrepancies cast serious doubt on the value of the VI survey.

Finally, Kjeldsen & Frandsen (1991) have published CCD photometry on the UB V system for 13 clusters, including IC 4651, with the primary motivation of looking for stellar variability. Their table of broad-band photometry has seven stars from IC 4651 in common with the photoelectric $uvbyH\beta$ survey; of these, 5 stars produce a mean residual in V , in the sense (ATT - KF), of $+0.041 \pm 0.008$. The zero-point shift is consistent with the approximate means used by KF to zero their photometry. Two of the stars, EG 65 and 76, exhibit residuals of -0.19 and -0.55 mag, respectively; similar residuals would result if our photometry is replaced by that of Mermilliod et al. (1995). Both deviants are red giants but EG 65 is also a spectroscopic binary (Mermilliod et al. 1995). Photographic and photoelectric observations of EG 76 are difficult because of potential contamination by a nearby star.

3. CCD DATA

3.1. Observations and Processing

New photometric data for IC 4651 were obtained in July of 1997 with the Cassegrain Focus CCD Imager and 0.9m telescope at the Cerro Tololo InterAmerican Observatory. For this run, the CCD was backed with a Tektronix 2048 x 2048 detector mounted at the $f/13.5$ focus of the telescope. The $0.40''$ unbinned pixels of the Tek chip provide for a generous field size of $13.5'$ by $13.5'$. The selected amplifier configuration yielded a true gain of approximately 3.2 electrons per adu. We used the 4-inch square $uvbyCa$ filters resident at Cerro Tololo and the $H\beta$ imaging filters of the same size borrowed from Kitt Peak National Observatory. Technical constraints made it impossible to mount all of these large filters on any given night; one unfortunate consequence of this constraint and the limited number of photometric nights was our failure to obtain any frames with CTIO's large imaging Ca filter.

Most of the Strömgren filters are so narrow that dome flats are difficult to obtain. Our general procedure has been to obtain dome flats for the redder and wider filters (y , b and $H\beta_w$), and augment these with sky flat observations if possible. We depended entirely on sky flats for the u , v and $H\beta_n$ filters. Color balance filters are impractical for intermediate-band dome flats; the narrow bandpass for these filters does allay somewhat the differences in continuum slope across the bandpass that results, in principle, from different color-temperatures between flat field lamps and the twilight sky.

A sizable sample of bias frames is routinely obtained in the afternoon and averaged with an imposed 3σ clip. Flat fields are typically fewer in number, 4 to 10, and are averaged following a modal scaling to accommodate different exposure levels. These calibration frames are applied to the incoming data frames within an IRAF-based routine, CCDPROC. We process and archive each frame and do not generally average repeated exposures.

In the most ideal circumstances, CCD photometry would be obtained on photometric nights in fields where each star is well separated from all neighbors; for such data, aperture magnitudes provide the best measurements of relative fluxes within frames and from frame-to-frame. Most cluster environments are too crowded to be treated so optimistically and relative fluxes among a large sample of stars on each frame must be obtained by profile-fitting algorithms. For our more crowded cluster fields, we obtained profile-fit magnitudes for each star above the sky level by some preset factor of the random error per pixel on each frame, using the ALLSTAR algorithms within DAOPHOT as found in IRAF releases. Beginning with an initial sample of 25 to 40 bright and relatively isolated stars, an initial point-spread-function (psf) is developed and used to clear the vicinity of the psf stars of neighbors; a more definitive psf is constructed from the partially cleaned frame using the best of the original candidates. After a number of preliminary passes through some of our data, we determined that it was advisable to use a spatially variable psf and routinely worked to parameterize a psf which includes a quadratic dependence on x and y .

Each frame yields instrumental magnitudes for thousands of stars, identified only by position. The instrumental magnitudes and associated errors for each frame are checked, and limits for inclusion in the composite average are defined based upon the error distribution with magnitude and the individual χ values defining the quality of the fit of the psf to the stellar image. We employ software which collates instrumental magnitudes for stars in a common field by identifying stars whose positions match to some preset threshold, typically one pixel or less. At an intermediate stage in this process, instrumental magnitudes for each star and from each frame of a similar color, are grouped in a large array. The next step in the process is to determine and remove any systematic difference between the magnitude scale of one frame and another; the array is then updated with

these corrected magnitudes for each star, on each frame of that color.

A final software step averages the magnitude entries for each star and in each color, constructs a standard error of the mean magnitude, and combines magnitudes to produce the desired indices. Unless a star has only one observation at a given color, the associated error of a magnitude or index is based primarily on the variation determined by frame-to-frame comparisons. The product of these software operations is a long file with magnitudes and indices for each star, internally precise and self-consistent to a high degree but not yet related to a standard system of magnitudes. That step requires measurements based on total flux for well-observed and spatially isolated stars within the program fields as well as carefully determined calibration equations.

Even in $2''$ seeing, a large fraction of the flux of a star lies within a radial aperture of 14 to 16 pixels radius. In a spirit akin to photoelectric photometry techniques, we have aimed for apertures of this size, surrounded by sky annuli with total area comparable to the central aperture area. As a check against crowding and contamination of the sky annuli, we generally impose a cut on the magnitude error offered by the aperture photometry algorithm and on the number of rejected sky pixels.

Aperture magnitudes are obtained for standards on photometric nights and for a number of sufficiently clean stars on each frame for each program object field observed on a photometric night. Magnitudes for similar colors are averaged without any additive correction other than for extinction and indices constructed. The difference between aperture-based and *psf*-based magnitudes and indices is determined for each program field.

3.2. Calibration to the Standard System: $H\beta$

Observations with $H\beta$ filters were obtained on two nights, 2 and 3 July, 1997, with the second of these two nights proving to be non-photometric. A brief discussion of the strategy for reduction of photometry to the standard system for these two nights of photometry will illustrate our typical procedure.

There are drawbacks to employing short exposures with a CCD camera and, if multiple frames for photoelectric standards are desired, standardization of CCD photometry can tax the patience of the most dedicated photometrist. Our compromise strategy combined observations of ten field $H\beta$ photoelectric standards with longer frames obtained in several open clusters with rich samples of stars observed on the $H\beta$ system.

Even on a non-photometric night, an open cluster field with numerous photoelectrically

observed stars can provide constraints on the fundamental slope linking instrumental $H\beta$ indices to standard values. We were able to utilize data obtained in two open clusters, NGC 4755 and NGC 3766, observed on a non-photometric night, as well as observations of field star standards and IC 4651 on the one photometric night.

Six $H\beta$ frames were obtained in NGC 3766 on a non-photometric night, with exposure times of 5 to 15 seconds for the $H\beta_w$ filter, 25 to 70 seconds for the $H\beta_n$ filter. The cluster field is comfortably uncrowded and aperture photometry was obtained for stars in common with photoelectric surveys by Shobbrook (1985; 1987). As absolute flux calibration would not be an issue, a relatively small aperture (10 pixels) was used. If more than 10 pixels were rejected from the annulus between 12 and 16 pixels around the star or if the aperture magnitude carried an error estimate greater than 0.10 mag, the measured magnitude was not included in the computation of the instrumental $H\beta$ index. Published V magnitudes were compared to $H\beta_w$ magnitudes to exclude mismatched and misidentified stars. A linear solution between instrumental and photoelectric $H\beta$ indices was derived for 25 stars with $H\beta$ indices between 2.58 and 2.78, with a resulting slope of 1.13 ± 0.07 in the sense $H\beta_{pe} = 1.13H\beta_{CCD} + a$. The scatter about this linear solution is small, ± 0.015 mag, so the uncertainty in the slope is presumably due to the modest numerical range in $H\beta$.

NGC 4755 is a rich field, in every sense of the word; several Strömrgren photometric surveys in the “Jewel Box” are available for comparison to CCD indices, including an early *uvby* $H\beta$ survey by Perry et al. (1976). This classic study formed the basis of Shobbrook’s (1984) expansion of *uvby* $H\beta$ photometry in this young cluster. Most recently, Balona & Koen (1994) have published CCD *uvby* $H\beta$ indices for 142 stars in this, the κ Crucis cluster, of which 121 were matched by position to stars measured on our frames.

With a large and potentially deep comparison in mind, our six frames in NGC 4755 were processed through profile-fitting algorithms to produce instrumental indices for over 300 stars. For the particular purpose of determining the slope of the relation between instrumental and standard $H\beta$ indices, we found that the large CCD-based sample of Balona & Koen (1994) and the older photometry of Perry et al. (1976) yielded linear comparisons inferior to a comparison to Shobbrook’s (1984) photoelectric data in the cluster. A linear fit between indices for 16 stars in common to both samples yields a tight (dispersion = ± 0.012) relation about a slope of 0.92 ± 0.04 in the same sense as the larger value cited for NGC 3766.

Both clusters are fairly young and the range of $H\beta$ indices similar. Assuming a zero-point offset between the two clusters’ relations between instrumental and photoelectric indices allowed us to merge the samples, producing a slope (not surprisingly) between these two values, in the sense $H\beta_{pe} = (1.05 \pm 0.04) H\beta_{CCD}$.

Although an older cluster, IC 4651 also incorporates a similar range of $H\beta$ indices among its brighter stars, between 2.58 and 2.85. Two photometric surveys were potential sources for photoelectric $H\beta$ indices; Nissen (1988) published $uvbyH\beta$ photometry for a number of open clusters, including $H\beta$ indices for 8 stars in IC 4651. Another survey with a larger sample is the $uvbyH\beta$ sample of Twarog et al. (1987). To maximize the internal consistency of this comparison and minimize the use of crowded images, this larger sample was employed without extension from the Nissen (1988) study.

Five frames of IC 4651 were obtained on the photometric night of July 2, 1997 and were examined for their contribution to the slope and the zero point of the $H\beta$ index calibration. All photoelectric standards on frames from this night were measured within 16 pixel apertures surrounded by a 5-pixel wide annulus. Any aperture measurement with more than 10 sky pixels rejected was excluded from the computed mean magnitudes. Fourteen stars in common with the photoelectric sample were selected for comparison to aperture magnitudes and indices. The slope implied by this comparison is 1.22 ± 0.04 .

One other set of data was brought to bear on the question of the slope and intercept of the calibration equation for $H\beta$ indices, the aperture magnitudes for 10 field $H\beta$ standards. Four bright stars are from the E-region standard compilations of Cousins (1989; 1990); six fainter stars ($V \sim 10.8$ to 13.5) were selected from south galactic cap A and F stars observed by Andersen & Jensen (1985). Results for these field stars are similar to the aggregate cluster surveys. All 10 stars yield a value for the slope between instrumental and standard $H\beta$ indices of 1.06 ± 0.03 , with a slightly steeper value, 1.14, implied by the six brightest stars.

The separate determinations were averaged, using the formal errors in the fitted slope as weights, to produce a composite transformation slope of 1.08 ± 0.02 . This slope was applied to all aperture-based $H\beta$ indices for the one photometric night to derive the necessary constant term in the calibration equation with a precision of ± 0.011 mag. The composite sample included 24 stars with $H\beta$ indices ranging from 2.58 to 2.88 in this determination.

3.3. Calibration to the Standard System: $uvby$

Our program design called for the observation of field star standards to provide the primary basis for the reduction of cluster observations to the standard $uvby$ system. To this end, ten field star dwarf standards with $(b - y)$ colors between 0.2 and 0.6 were observed on 4 July 1997, one of them at widely separated airmass to establish airmass corrections.

For several reasons, we modified plans for these reductions. A major priority of the July 1997 observational program was a study of the main sequences of nearby globular clusters; for that reason, the selected field star standards are primarily metal-poor dwarfs drawn from the sample of Schuster & Nissen (1988). This sample provides a far-from-ideal match to IC 4651 members, particularly with respect to the m_1 indices. This circumstance, plus the existence of *uvby* photoelectric observations in the field of IC 4651, argues for an additional appeal to the photoelectric photometry described in Section 2 for potential adjustments to the zero points of the calibration equations.

It also appeared helpful to make use of a larger sample of data to characterize the color terms which particularly affect the reduction of instrumental m_i indices to standard m_1 values. Because an intrinsic correlation exists between a limited range of m_1 and $(b - y)$ values for the field dwarf standards, it may be hard to disentangle a potential instrumental signature of a color term for m_1 . We used a comparison of published photometry in IC 4651 (Anthony-Twarog & Twarog 1987) to frames obtained on 4 July and 5 July 1997 and to data obtained in a field of M67 with an identical experimental setup in February 1998, using the photometry of Nissen et al. (1987) for comparison. It may be noted that frames from a non-photometric night may assist in determining color terms if a broad enough range in parameter space (temperature, metallicity and luminosity class) may be explored.

Each standard star was measured on each frame obtained on 4 July 1997 within a large (14 pixel radius) aperture, surrounded by a sky annulus of comparable area. Following corrections for atmospheric extinction to magnitudes obtained from each frame, instrumental indices were compared to standard indices in separate solution classes. Dwarfs were divided at $(b - y) = 0.42$ for separate solutions; no giant field standards were observed, so that the calibration of photometric indices for evolved stars in IC 4651 is entirely based on the photoelectric photometry discussed in Section 2.

Table 2 summarizes the slope and color terms which characterize each derived calibration equation applicable to the aperture-based indices. The calibration equation for m_1 , for example, is of the form:

$$m_1 = a_m m_i + c_m (b - y)_i + b_m$$

where m_i and $(b - y)_i$ refer to the instrumental indices. The number of stars contributing to each set of coefficients is noted, as well as the standard deviation describing the scatter of calibrated indices about standard values.

The coefficients for the red giant solution are rather noisy, due in part to small numerical ranges for m_1 and c_1 ; this solution was determined by direct comparison of photoelectric indices to the *psf*-based indices for stars redder than $(b - y) \sim 0.5$ and with c_1

larger than ~ 0.40 .

Eight frames had been obtained in IC 4651 on the same photometric night as the standard stars, and were analyzed in a similar manner so that magnitudes and indices on the standard system should be readily obtainable for relatively isolated stars in the cluster field. Twenty such stars were selected for measurement from the sample of stars with revised photoelectric indices. Aperture-based indices for these 20 stars were directly compared to the instrumental indices derived from *psf*-fits. Most of the 3904 stars measured in the IC 4651 field are too crowded for effective aperture photometry; with the mean difference between *psf*-based and aperture-based indices determined and removed, the entire set of photometry can be calibrated with the equations described in Table 2. These mean differences, determined from 20 stars, carry standard deviations of 0.007, 0.007, 0.012 and 0.010 for V , $(b - y)$, m_1 and c_1 respectively.

As a final check on the calibrated CCD photometry, differences between the CCD data and the photoelectric data of Nissen (1988) and Anthony-Twarog & Twarog (1987) were constructed. Nine stars measured by Nissen (1988) have m_1 and c_1 indices that may be compared; an additional star has V and $(b - y)$ data in both samples. The differences, in the sense (photoelectric - CCD) are 0.001 ± 0.020 , -0.016 ± 0.019 , 0.030 ± 0.034 and -0.010 ± 0.022 for V , $(b - y)$, m_1 and c_1 . The corresponding differences for 43 stars in common with the Anthony-Twarog & Twarog (1987) sample are 0.002 ± 0.018 , -0.010 ± 0.018 , 0.040 ± 0.043 , and 0.005 ± 0.022 . Corrections of 0.001 mag have been applied to the calibrated CCD V magnitudes, -0.013 to the $(b - y)$ colors, 0.035 to m_1 and -0.003 to c_1 . The sizable correction to the CCD calibrated m_1 index validates our concern about the marginal suitability of the metal-poor field star standards which underly the CCD calibration.

We note here also an explicit comparison of calibrated $H\beta$ indices for 14 stars with photoelectric $H\beta$ photometry from Anthony-Twarog & Twarog (1987); the mean difference in the sense (photoelectric - CCD) is -0.002 ± 0.015 .

Table 3 lists the full set of photometry for the IC 4651 field, based on analysis of 6 y frames, 6 b frames, 2 v and u frames, 8 $H\beta_w$ frames and 7 $H\beta_n$ frames. A few stars appear to be giants but could not be classified as such, either because there was no c_1 index or, as in the case of the putative barium star EG 23, the c_1 index gives a misleading result; these stars' indices are italicized as an indication that the calibration equations for giants were applied. We transformed our x and y CCD coordinates to the common system defined for the cluster in the WEBDA data compilation (Mermilliod 1998). The scale for this coordinate system, centered on the star EG 56, is approximately 3.2 arcseconds per unit. Stars with EG identifications are explicitly marked; other cross-identifications may be

made by comparison to the web-based compilation for which identifications may be found in the first column.

4. CLUSTER PARAMETERS

As discussed in Sec. 1, the ultimate goal of this photometric program is to determine with the highest precision possible the fundamental cluster parameters of reddening, metallicity, and distance. In an ideal setting, one would have proper-motion and radial-velocity membership information which allowed the observer to isolate a sample minimally contaminated by field interlopers. Moreover, identification of binaries would permit the elimination of stars whose structure and evolution may have been altered by their duplicitous nature. In short, the cluster properties could be obtained from as pure and representative a sample as possible (see, e.g., Daniel et al. 1994; Nordström et al. 1997). For globular clusters, one can often sidestep these issues due to the paucity of binaries outside of the cluster core and the high ratio of cluster members to field stars within the tidal radius.

Open clusters, unfortunately, are a different matter. They are often poorly populated and, as distance and/or age increase, the brightest stars at the cluster turnoff are more readily lost against the rich background of disk stars. As time passes, the initially rich population of cooler dwarfs may be tidally stripped from the cluster leaving few, if any, of the lower mass stars, assuming the cluster as a whole survives. In the absence of the type of detailed information noted above, a more pragmatic approach is required, optimizing what is more easily obtainable, an extensive array of very accurate magnitudes and color indices. The ultimate product of the approach which follows is a sample of stars which is composed purely of cluster members with photometric indices of high precision. The sample should be restricted to unevolved main sequence stars and stars near the cluster turnoff. As will become apparent below, the completeness of the sample is irrelevant; all that matters is that non-member contamination of the sample be minimized. Keeping non-members out is more important than keeping members in. Finally, the underlying principle which determines the success of the technique is that the cluster members are homogeneous in age and composition.

Before applying the constraints to IC 4651, we note that this cluster is not typical of the objects which will be analyzed in later papers in the sense that it was observed for use as a calibration cluster. The frames were not taken with exposure times designed to reach fainter magnitudes but merely to V brighter than 13 where the photoelectric observations were located. Moreover, the number of u and v frames is a factor of four smaller than that

typical of our program clusters, again limiting the high accuracy photometry to the brighter stars.

4.1. Thinning the Herd: the Color-Magnitude and Color-Color Diagrams

To illustrate the nature of the problem, we present in Fig. 1 the CMD for IC 4651, using $(b - y)$ as the temperature index. The sample has been restricted to include only stars with at least two observations each in b and y . For $(b - y)$ less than 0.6 and V brighter than 14, it is obvious that cluster stars dominate. For stars fainter than $V = 15$, the contribution by the field star population is significant for $(b - y)$ redder than 0.4, and increasingly dominates at fainter magnitudes. In fact, the cluster CMD virtually disappears in the sea of background stars at fainter magnitudes. We note that the broad distribution of fainter stars is not a product of photometric errors. As illustrated in Fig. 2, the dispersion in $(b - y)$ remains typically below 0.05 mag to almost $V = 18.0$. The high accuracy of the photometry allows us to make a second cut to reduce the sample further; only stars with a standard error of the mean in $(b - y) \leq 0.010$ will be analyzed. The CMD resulting from this cut is shown in Fig. 3.

The expanded scale, coupled with the removal of stars with larger photometric errors, provides more insight into the CMD structure. It is now possible to see the outline of the probable cluster main sequence between $V = 15$ and 16, as well as an upper boundary defined by potential binaries approximately 0.75 mag above the main sequence. However, there is no question that the stars fainter than $V = 12$ and redder than $(b - y) = 0.65$ are field interlopers. Keeping in mind our precept to avoid field stars and anomalous cluster members whenever possible, the next major restrictions on the sample will limit the analysis to stars between $V = 11$ and 14.6 and $(b - y)$ between 0.30 and 0.5. The bright limit removes the giants from consideration while the blue limit excludes the blue stragglers. The faint and red limits cut out the field star population that emerges near $(b - y) = 0.42$ while the red bound allows potential cooler, main-sequence binaries to be retained.

Since the sample has been restricted to stars whose position within the CMD is consistent with membership, additional constraints must come from additional information. We make use of the color-color diagrams, specifically $c_1, (b - y)$. For the stars of interest, the c_1 index is a surface gravity indicator and can separate dwarfs from subgiants and giants. To maintain our accuracy standards, the sample will be restricted to all stars with at least two observations each in v, u , and, for future purposes, $H\beta_w$ and $H\beta_n$. Moreover, all stars with standard errors of the mean greater than 0.015 in m_1 or c_1 , or 0.010 in $H\beta$ will be excluded. The resulting $c_1, (b - y)$ diagram is shown in Fig. 4. The form of the

mean relation for the cluster is apparent, with c_1 increasing steadily along the unevolved main sequence as $(b - y)$ decreases. The vertical band at the turnoff in Fig. 3 is reflected in the rise in c_1 , followed by a turnover in c_1 as $(b - y)$ increases among the evolved stars in the red hook and subgiant branch. The selection criterion here is that stars that lie above the c_1 -relation defined by the main sequence stars must be there because they are evolved or because photometric errors have shifted them away from the main sequence relation. If the former case is true and the stars are members, their evolved status should be reflected in the traditional CMD; if not, they may be classified as field stars. If their anomalous location is the product of photometric scatter, they should be excluded whether they are members or not. Note that, as discussed in Twarog (1983), deviations above the unevolved color-color relation cannot be explained by binarity among the main sequence stars. In Fig. 4, filled symbols tag stars identified as being evolved; separation of evolved versus unevolved is limited to stars redder than $(b - y) = 0.37$. We have also tagged with crosses the two stars with unusually high c_1 .

Fig. 5 illustrates how this information may be used. The symbols have the same definition as in Fig. 4. Among the brighter sample, with one exception, all the stars whose positions in the CMD would classify them as evolved have been tagged as such by the c_1 criterion. The one star near $(b - y) = 0.45$ is a probable field dwarf interloper in front of the cluster. Among the fainter stars, the majority of the stars classed as evolved scatter away from the unevolved main sequence. Though their CMD position might indicate binarity for some of the discrepant stars, this explanation is inconsistent with the c_1 data. The majority of these stars are likely distant subgiant and giant interlopers. For the one star at $(b - y) = 0.38$ that lies near the main sequence, photometric scatter is the likely source of its anomalous classification. It barely meets the c_1 criterion for classification as evolved and previous photometry of this star (Anthony-Twarog & Twarog 1987) places it clearly among the unevolved cluster members on the $uvby$ system. Finally, the two stars with high c_1 values (crosses) have positions in the CMD inconsistent with cluster membership given their c_1 indices. Excluding all the probable interlopers and photometric anomalies leaves us with a sample of 98 stars, binaries included.

4.2. Reddening and Metallicity

Determination of these two fundamental parameters is coupled when following the $uvbyH\beta$ approach. $H\beta$ defines the intrinsic color of the star under the assumption that it is an unevolved star with Hyades abundance. This intrinsic color is then modified to adjust for the effect of evolutionary and abundance differences using a variety of terms linked to

δm_0 ($m_{0stan} - m_{0star}$) and δc_0 ($c_{0star} - c_{0stan}$). The intrinsic $(b - y)_0$ is compared with the observed value to produce the star’s reddening, $E(b - y)$. However, the initial indices used to define $(b - y)_0$ include reddening, so the standard method is to correct the original indices with the estimated reddening and iterate the procedure until the reddening converges.

The primary weakness in the approach for single stars is that, except for $H\beta$, the key indices of $(b - y)$, m_1 , and c_1 are linked through common filter combinations. Thus, a photometric error in one or more of the magnitudes produces correlated errors among the indices, potentially enhancing the errors in the reddening and metallicity estimation. In contrast, the stars in a cluster have a common metallicity and, hopefully, uniform reddening. By combining the data for a large, homogeneous sample, one can define a composite value for the cluster which can be adopted for every star, rather than using the individual values derived for each star. The procedure, as outlined in Nissen et al. (1987) and Anthony-Twarog & Twarog (1987), is to derive the cluster reddening under various assumptions for the metallicity, i.e., δm_0 , then derive the cluster metallicity under different assumptions for the reddening, $E(b - y)$. As the metallicity is lowered (δm_0 increases), the derived reddening increases because the stars are intrinsically bluer; as $E(b - y)$ is increased, the derived metallicity increases primarily because the reddening correction makes m_0 larger. Comparison of these two trends results in a unique combination of $E(b - y)$ and $[Fe/H]$ where the two relations cross.

The remaining option is the selection of the intrinsic color relation, the two primary choices being that of Olsen (1988) and that of Nissen (1988) based upon a modified version of the Crawford (1975) relation. For comparison purposes and to link our results to the extensive cluster sample of Nissen (1988), we will include both. As we show below, the choice of the intrinsic color relation does affect the final cluster values.

One additional change comes from the improvement in the quality and quantity of the photometric data. In earlier work, δm_0 and δc_0 were defined by comparison to the standard values of the star at the same $(b - y)_0$, rather than the same $H\beta$. This was done because not all stars had $H\beta$ photometry and the photometric accuracy of $(b - y)$ was invariably higher than that of $H\beta$. A pseudo- $H\beta$ index was created from $(b - y)$ by adjusting the color to what it would have been if the star had Hyades metallicity using the modest offset recommended by Crawford (1975). For a cluster like IC 4651, which is known to have a metallicity comparable to the Hyades, the color adjustments are at the level of a few millimagnitudes. As an internal check on the photometric reliability, we have done the simultaneous fit of the reddening and metallicity using both $(b - y)$ and $H\beta$ as the primary temperature index.

For the 98 stars classed as probable cluster members, as the metallicity of IC 4651

is varied from $+0.12$ to -0.10 , the intrinsic color relation of Olsen (1988) yields $E(b - y)$ between 0.060 ± 0.023 to 0.070 ± 0.022 , where the errors quoted are the standard deviations for a single star. For the abundance estimate we vary the reddening from $E(b - y) = 0.080$ to 0.070 to 0.060 . Excluding the only two stars to lie more than three sigma from the cluster mean, from 96 stars, $[\text{Fe}/\text{H}]$ ranges from $+0.137 \pm 0.127$ to $+0.098 \pm 0.119$ to $+0.066 \pm 0.110$ for the $\text{H}\beta$ index and $+0.192 \pm 0.116$ to $+0.131 \pm 0.103$ to $+0.078 \pm 0.104$ for the adjusted $(b - y)$ index. Taking both estimates into account, the final estimates for the cluster are $E(b - y) = 0.062 \pm 0.003$ and $[\text{Fe}/\text{H}] = +0.077 \pm 0.012$, where the quoted errors now refer to the standard error of the mean as defined by internal errors alone. In contrast, if we use the same intrinsic color relation of Nissen (1988), the reddening rises to $E(b - y) = 0.071$ and $[\text{Fe}/\text{H}]$ increases to $+0.115$, accordingly.

An alternative method of deriving the reddening that doesn't require a priori estimates of the metallicity is available from the work of Schuster & Nissen (1989). The intrinsic $(b - y)$ for a star is derived from the $\text{H}\beta$ index, but is modified for evolutionary and metallicity effects using the actual m_1 and c_1 values, rather than the differences compared to a standard sequence. The process still requires multiple iterations to adjust for reddening. Applying this calibration to the 98 stars in IC 4651, one gets $E(b - y) = 0.039 \pm 0.012$ (s.d.). Though the scatter is significantly smaller, the reddening is significantly lower. Fortunately, this difference in $E(b - y)$ is expected and has been discussed by Schuster & Nissen (1989). The focus of the revised calibration is the population of stars of intermediate and low $[\text{Fe}/\text{H}]$, predominantly those below $[\text{Fe}/\text{H}] = -0.5$. Thus, the number of calibrators at hotter temperatures with solar abundance and higher is small and the alternate calibration generally produces an underestimate of $E(b - y)$ for metal-rich stars when compared with the Olsen (1988) color relation. However, as a check on the metallicity, we can fix the reddening at $E(b - y) = 0.062$ and apply the $[\text{Fe}/\text{H}]$ calibration of Schuster & Nissen (1989). Excluding the four stars that lie more than three sigma from the cluster mean, $[\text{Fe}/\text{H}] = +0.099 \pm 0.145$ (s.d.), in excellent agreement with the value derived above.

How do the new values compare with previous results? A complete discussion of the results as of 1988 may be found in Anthony-Twarog & Twarog (1987). The reddening of $E(b - y) = 0.062$ is the same within the errors as found from a much smaller sample of *wby* $\text{H}\beta$ photoelectric data in Anthony-Twarog & Twarog (1987). It is less than the $E(b - y)$ of 0.076 found from 8 stars by Nissen (1988), but the correct value for comparison is $E(b - y) = 0.071$ obtained when the same intrinsic color relation is adopted. The remaining portion of the difference is due to slight differences in the zero points for $\text{H}\beta$ and $(b - y)$. The lower $[\text{Fe}/\text{H}]$ relative to the value of $+0.18$ found by Nissen (1988) is a combination of the lower adopted reddening and a small difference in the photometric zero points.

The only additional abundance estimate is the DDO value from TAAT. Assuming $E(B - V) = 0.12$ for the main sequence stars, DDO of the giants produces $[\text{Fe}/\text{H}] = 0.09 \pm 0.02$ (s.e.m.); lowering the main sequence reddening to $E(B - V) = 0.085$, equivalent to the $E(b - y) = 0.062$, lowers the DDO abundance to $[\text{Fe}/\text{H}] = 0.06$. The DDO and *wby*H β estimates appear to be totally consistent for this cluster.

4.3. Distance and Age

Though the availability of c_1 permits a photometric distance determination, the quality and quantity of the main sequence $V, (b - y)$ photometry allows an even more reliable distance estimate from main sequence fitting. The approach adopted here follows the treatment by Nordström et al. (1997) for NGC 3680, with the advantage of a more richly populated main sequence in IC 4651.

IC 4651 has a metal abundance similar to the Hyades cluster, a coincidence which argues for a direct fit to the Hyades main sequence to determine IC 4651’s distance. Strömberg photometry in the Hyades is available from studies by Crawford & Perry (1966) as well as from the catalog of Olsen (1993). As the Hyades cluster is near enough to neglect reddening, observed colors may be considered equivalent to reddening-free indices. Nordström et al. (1997) referred to a convergent point analysis of Hyades proper motions by Schwan (1991) as a source for individual distance moduli and subsequent absolute magnitudes; we have opted to use the more recent Hipparcos-based parallaxes in Perryman et al. (1998) from which a mean cluster distance modulus of 3.33 ± 0.01 is derived. Collating individually-derived absolute magnitudes and colors for confirmed member stars produces a list of over 100 Hyades members.

A comparison of the cluster main sequences is presented in Fig. 6 where 0.062 has been added to the colors of the Hyades stars to match the IC 4651 cluster reddening of $E(b - y) = 0.062$, and 10.15 has been added to the Hyades absolute magnitudes to simulate the effect of IC 4651’s apparent distance modulus. Different symbol types distinguish stars with colors from the two photometric sources. If the reddening is increased to $E(b - y) = 0.071$ and $[\text{Fe}/\text{H}]$ rises, the apparent modulus rises to just under 10.3.

Clearly, IC 4651 is older than the Hyades cluster and evolution has caused the bluer portion of the main sequence of IC 4651 to increasingly deviate from the less evolved main sequence of the Hyades. However, a quantitative estimate of the age differential requires comparison to a set of isochrones. The isochrones, in turn, must be consistent with the chemical composition of the program stars to as great an extent as possible. As a starting

point, we have selected the models of Bertelli et al. (1994), which include the effects of convective core overshoot and have been shown, most recently in Twarog et al. (1999), to reproduce to a high degree the morphology of observed clusters near the cmd turnoff when the models are properly zeroed in the observational plane. Following the precepts of Nordström et al. (1997), we have adopted the conversion of luminosity to absolute magnitude without revision. Effective temperatures have been converted to $(b - y)$ using a color-temperature relation derived in Edvardsson et al. (1993) for stars with $[\text{Fe}/\text{H}] \sim 0.10$; this again mimics the treatment of NGC 3680 stars by Nordström et al. (1997) but imposes a restriction on the applicable color range for this transformation of $(b - y)$ between 0.25 and 0.45.

Figure 7 shows the superposition of the absolute CMD for Hyades members and the unevolved main sequence of an isochrone for $Z = 0.02$ and an age of 0.8 Gyr from Bertelli et al. (1994). The excellent agreement between the unevolved main sequences provides reassurance that the absolute magnitudes and colors of the transformed isochrones are a good fit to clusters with similar compositions.

The final step in the process is illustrated in Fig. 8. Isochrones for ages 1.6 and 2.0 Gyr have been transformed to the observational plane with additional shifts of 10.15 and 0.062 in V and $(b - y)$, to match the observed indices for IC 4651 stars. The position and shape of the turnoff and red hook are an excellent match to the isochrones, implying an age of 1.7 Gyr with an uncertainty below 0.1 Gyr. Beyond the turnoff, the two subgiants are slightly brighter than predicted, but no information is currently available regarding the possibility of a binary nature. Raising the reddening to $E(b - y) = 0.071$ lowers the cluster age by about 0.1 Gyr while raising the apparent modulus to just under 10.3. We note that while the isochrones provide an ideal match to the CMD morphology, the *absolute* age is ultimately tied to the zero point of the transformations between the observational and theoretical planes and the link between stellar color and mass, as discussed in Twarog et al. (1999).

Returning to the question of using c_0 versus $(b - y)_0$ or $\text{H}\beta$ to derive distances, we refer to the comparison in Fig. 9. Plotted as open circles are the data for the Hyades (Crawford & Perry 1966) while the filled triangles are the stars in IC 4651, adjusted for a reddening of $E(b - y) = 0.062$. The agreement between these clusters in the unevolved portion of the color-color diagram is encouraging and consistent with the comparison from Fig. 6. If we require that IC 4651 superpose with the Hyades, the uncertainty in the combination of the zero-point for c_1 and the reddening estimate must be less than 0.005 mag. The claim that the two should superpose is not guaranteed because of the effect known as the Hyades anomaly (see Nissen 1988 and references therein). The anomaly

with the Hyades is that despite the fact that c_0 at a given $H\beta$ should be the same for all unevolved stars in the F stars regime, the Hyades main sequence lies approximately 0.03 magnitudes above the standard relation defined by field stars in the solar neighborhood. The work of Nissen (1988) has demonstrated convincingly that this problem is not unique to the Hyades, appearing to a larger degree in Praesepe and to a lesser degree in NGC 2287 and NGC 2301. Though IC 4651 was included in the Nissen (1988) survey, none of the stars observed were on the unevolved main sequence. With the current data, it appears that IC 4651 also exhibits c_0 indices which are too large by between 0.025 and 0.035 mag relative to the nearby field stars, though the discrepancy is reduced if the larger reddening value is adopted. Comparison to the standard sequence will lead to a δc_0 measure of 0.03 which, at the redder colors of the unevolved main sequence, could produce an overestimate of the cluster distance between 0.4 and 0.6 mag, assuming the standard relation should apply to the cluster. A direct check of the distance discrepancy between the photometric value and that from main-sequence fitting indicates a more typical discrepancy between 0.2 and 0.4 mag (Nissen 1988). Photometric distances using $uvbyH\beta$ with no adjustment for the anomaly range from $(m - M) = 10.1$ for Anthony-Twarog & Twarog (1987) to 9.7 for Nissen (1988), though the stars used in the determinations were evolved stars at the turnoff. The photometric zero-point differential for c_1 is the primary source of the offset between the two studies.

How do the modulus and age estimates compare with previous values? The main sequence fit by TAAT, which supersedes the earlier isochrone match in Anthony-Twarog et al. (1988), leads to $(m - M) = 10.25$ under the assumption of $E(B - V) = 0.12$ ($E(b - y) = 0.088$) and a metallicity virtually identical to the value derived above. Adjustment for the lower reddening reduces this to $(m - M) = 10.1$, in good agreement with the $(b - y)$ fit to the Hyades and the transformed isochrones. The type and size of the change in the derived modulus from the earlier value in TAAT are typical of the effect expected in comparisons with other analyses. Superposed in the studies that use isochrone matches are the differences in the assumed solar color for the isochrones and the failure to adequately transform from the theoretical to the observational plane. These differences also translate into differences in the derived ages. Anthony-Twarog et al. (1988), Anthony-Twarog & Twarog (1987), and Kjeldsen & Frandsen (1991) get an age of about 2.4 Gyr for IC 4651 using isochrones which failed to include convective overshoot. The reduction in age with newer isochrones when overshoot is included is a now familiar pattern first noted in the discussion of the age of NGC 5822 (Twarog et al. 1993) and confirmed with the analysis of NGC 752 (Daniel et al. 1994). There appears to be little doubt regarding the need to include overshoot in the models for stars of intermediate mass; the primary issues under debate are the size and mass dependence of the mechanism (see, e.g., Kozhurina-Platais

et al. 1997; Rosvick & Vandenberg 1998; Pols et al. 1998). Using models with overshoot, Meynet et al. (1993) adopt $E(B - V) = 0.14$ to derive an age of 1.9 Gyr with $(m - M) = 9.9$. Lowering the reddening should decrease the modulus and increase the age but, as discussed in Twarog et al. (1999), when these isochrones are zeroed to the solar $(B - V)$ assumed in TAAT, the ages are reduced and the distances increase by approximately 0.35 mag. Carraro & Chiosi (1994) have used the same models adopted in this investigation with $E(B - V) = 0.10$ to get $(m - M) = 10.2$ and an age of 1.6 Gyr. However, they also assumed $[\text{Fe}/\text{H}] = -0.16$, which should lead to an underestimate of the distance and an overestimate for the age, both of which should be partially compensated by the slight overestimate of the reddening. Most recently, Pols et al. (1998) have found an excellent match to overshoot isochrones with $E(B - V) = 0.08$, $(m - M) = 10.0$, $[\text{Fe}/\text{H}] = 0.18$ and an age of 1.66 Gyr. In short, within the uncertainties of the zero-points for the isochrone transformations, adopting comparable values for reddening and metallicity produces an age between 1.5 and 1.7 Gyr for IC 4651, in excellent agreement with the current result.

An additional check on the distance modulus is provided by the giant branch, shown in Fig. 10 with $(b - y)$ as the temperature index. Filled circles are radial-velocity members of the cluster which do not exhibit evidence of binarity, open circles are probable binary members, and the starred symbols are stars for which radial-velocity data are unavailable. The classifications are taken from the survey of the cluster giant branch by Mermilliod et al. (1995). Three of the outer giants in the radial-velocity survey were beyond the CCD field; their $[B - V]$ values from Mermilliod et al. (1995) have been transformed to $(b - y)$ using a linear relation defined by the remaining 13 giants that overlap in color. As expected given the agreement between the two sets of photometry and the high internal accuracy of both, Fig. 10 reproduces the red giant clump structure seen in Fig. 11 of Mermilliod et al. (1995). The clump is richly populated, but extends in a vertical band between $V = 10.6$ and 11.0, with the brighter stars lying blueward of the clump. Though there is a significant range in V among the clump giants, if the distribution is analyzed using the approach commonly adopted for rich clusters, there is a definite peak in the sample at $V = 10.9 \pm 0.05$. However, the asymmetry in the luminosity distribution toward brighter stars could easily lead to a choice of $V = 10.8$ as more typical of the mean magnitude of the clump. With the lower reddening, this leads to M_V between 0.75 and 0.65 for the clump, decreasing to between 0.6 and 0.5 if $E(b - y) = 0.071$ is adopted, consistent within the uncertainty with values typical of open clusters of intermediate age with distances tied to main sequence fitting (TAAT). Use of an apparent modulus below 9.9 would make the clump in IC 4651 anomalously faint for its age.

To close our discussion of the CMD, we make one final comparison. Along with NGC 752 and IC 4651, the open cluster NGC 3680 has been the focus of a variety of

investigations to test the role of convective overshoot in intermediate-age open clusters. With each analysis, the quantity and quality of the data for this cluster have improved (Nissen 1988; Anthony-Twarog et al. 1989; Anthony-Twarog et al. 1991; Nordström et al. 1996), culminating in the discussions by Nordström et al. (1997) and Kozhurina-Platais et al. (1997). The last study is particularly important in that it includes precision BV photometry for an extended sample of stars in the cluster field which have proper motions indicative of membership. Nordström et al. (1997) supply CCD $(b - y)$ data for a number of these stars, but do not cover a comparable area of the sky, leading to a short supply of fainter cluster members. To make optimal use of the published data, we have used 48 stars brighter than $V = 15$ in NGC 3680 for which $(b - y)$ and $(B - V)$ data are available to define a linear transformation from $(B - V)$ to $(b - y)$ and converted $(B - V)$ for all the cluster members in Kozhurina-Platais et al. (1997) to the $(b - y)$ system. To account for a difference in reddening as implied by the internal comparison in Nissen (1988), the CMD for NGC 3680 was shifted by +0.04 in $(b - y)$. *No adjustment has been made to V .* The resulting composite CMD is presented in Fig. 11; crosses are stars in IC 4651, with starred points among the giants to identify binary members. Filled circles are stars in NGC 3680, while open circles are probable binaries as identified in Nordström et al. (1996). It should be remembered that binary information isn't available for all the stars, so the absence of a binary symbol does not imply absence of a binary. The agreement among the turnoff stars is exceptional while the clump stars of NGC 3680, few that there are, superpose nicely on the richer clump of IC 4651.

The implications of this are straightforward. NGC 3680 and IC 4651, known to have the similar $[\text{Fe}/\text{H}]$ as defined by the $uvby$ system, have identical ages and apparent moduli, while $E(b - y)_{4651} = E(b - y)_{3680} + 0.04$. However, despite the internal agreement, the absolute comparisons appear discrepant. With $E(b - y) = 0.034$ from the Nissen (1988) intrinsic color relation, Nordström et al. (1997) derive $(m - M) = 10.65$ from a direct fit to the Hyades based upon one star on the unevolved main sequence. Adjusting for an assumed Hyades modulus of 3.33 instead of 3.4 lowers this to 10.58, still too large compared to 10.3 for IC 4651 with an analogous reddening determination. However, using a comparison to a variety of theoretical isochrones, Nordström et al. (1997) do derive a modulus 0.25 mag smaller than that based upon the Hyades fit. Kozhurina-Platais et al. (1997) fit NGC 3680 to overshoot isochrones and get $(m - M) = 10.50$, assuming $E(B - V) = 0.075$. If we lower the reddening to $E(B - V) = 0.05$, the apparent modulus becomes 10.36, in good agreement with the current investigation. If, as suggested by a number of studies, the reddening for NGC 3680 is higher than $E(b - y) = 0.034$ ($E(B - V) = 0.047$) and, thus, $E(b - y)$ for IC 4651 is greater than 0.074, $(m - M)$ must be 10.3 or higher for both clusters and the red giant clumps must be at $M_V = 0.6$ or brighter.

5. SUMMARY AND CONCLUSIONS

Over the last 15 years advances in CCD technology and in the software and the hardware to process the data generated by the technology have escalated the rate at which information on large stellar samples can be obtained. Broad-band data on a multitude of systems, with an increasing emphasis on *VRI* photometry, has been used to survey and to study in detail an expanded sample of open clusters at magnitude levels once considered impossible for telescopes of modest size (see, e.g., Phelps & Janes 1994; Marconi et al. 1997; Tosi et al. 1998). Particularly important has been the transition to larger format CCD's, given the often sparse population of many open clusters.

Despite these changes, one of the tools which has lagged behind is the application of intermediate and narrow-band photometric systems to clusters. Early attempts focused on small fields using chips with responses that were poorly matched to the standard system, as well as a limited number of usable standards (e.g., Anthony-Twarog 1987; Anthony-Twarog et al. 1989). The latter issue was often overcome through the study of clusters which contained photoelectric observations which could be used to internally calibrate the CCD data, as in IC 4651 (Anthony-Twarog & Twarog 1987) and NGC 3766 (Balona & Koen 1994). Though there has been some movement toward greater use of CCD *uvbyH β* photometry (Nordström et al. 1996; Grundahl et al. 1998), the growth of the cluster data in this area remains remarkably slow. This is especially surprising given the facility with which one can disentangle the effects of temperature, surface gravity, and metallicity for stars which are generally common and of modest luminosity within most clusters. The inclusion of $H\beta$ provides a direct estimate of the reddening to each star which is almost independent of surface gravity and metallicity, making it less susceptible to assumptions about the similarity of nearby and distant stellar populations. In short, if the photometric accuracy required can be attained, *uvbyH β* provides an ideal method for deriving the fundamental cluster properties of reddening, metallicity, distance, and, indirectly, age.

In this paper we have presented CCD data for the intermediate-age open cluster, IC 4651, with the intention of illustrating the capabilities of even a simple application of the photometric approach to a reasonably well-studied object. Moreover, because of the large number of internal photoelectric observations, the CCD data for the cluster will serve as a regular tie-in to the standard system over the course of this program, i.e., it will be one of our standard clusters. Our expectation is that as more data are collected for IC 4651 and additional clusters with internal photoelectric observations are linked to IC 4651, the IC 4651 data will be periodically revised and expanded, leading to greater accuracy and a deeper limiting magnitude than permitted by the current modest set of frames. Future papers in this series will deal with a mixture of both program and standard clusters with the

ultimate goal of better delineating the galactocentric dependence of the cluster parameters (TAAT).

By restricting the photometric sample to stars with multiple frames in every filter with final photometric indices that have uncertainties of ± 0.015 or less in every index and by using the CMD and color-color diagrams to isolate highly probable cluster members in the F-star temperature range, one arrives at a definitive sample of 98 stars in IC 4651. From this sample, one derives $E(b - y) = 0.062 (0.071) \pm 0.003$ and $[\text{Fe}/\text{H}] = +0.077 (+0.115) \pm 0.012$, using the intrinsic color relation of Olsen (1988) (Nissen 1988), where the errors quoted are the standard errors of the mean and include internal errors alone. What this implies is that the only significant limit to the final accuracy of the relative cluster parameters of reddening and metallicity is the accuracy of the tie-in between the CCD data and the standard system. For IC 4651, the uncertainties in the cluster parameters are easily dominated by the ± 0.005 mag and ± 0.007 mag uncertainty in the photoelectric zero-points for m_1 and c_1 , respectively.

Given the reddening and metallicity, a direct fit to the Hyades main sequence using the Hipparcos-based modulus of 3.33 produces $(m - M) = 10.15$, while a higher reddening gives 10.3. The overshoot isochrones of Bertelli et al. (1994), checked to assure an appropriate match to the unevolved main sequence of the Hyades, produce, as required, the same modulus, but an age of 1.7 ± 0.1 Gyr for the cluster, as well as an excellent match to the morphology of the turnoff. This age estimate is consistent, within the uncertainties of the models and the transformations to the observational plane, with the published results for other isochrone compilations which include overshoot when applied to IC 4651 and adjusted for a common reddening. Obviously a higher assumed value for $E(b - y)$ leads to a younger age. As for the distance, there are few things one can do which will make the modulus smaller. If the reddening estimate and/or the metallicity are increased, which would be consistent with a number of past discussions of this cluster's parameters and the comparison with NGC 3680, $(m - M)$ becomes larger. Given the direct match of the cluster to the Hyades as in Fig. 6 and the low reddening value adopted, it is difficult to see how the distance could be less than $(m - M) = 10.1$. Despite the failure of the red giant clump to occupy a narrow luminosity range, a common property for clusters of this age, the derived modulus implies a maximum clump absolute magnitude between 0.8 and 0.7, with a more probable value near 0.5. Any attempt to shorten $(m - M)$ below 10.1 must address the resulting anomalous location for the clump and the discrepant link to NGC 3680.

We are grateful to Kitt Peak National Observatory for the loan of imaging H β filters and to Jim DeVeney, in particular, for his gracious help with those arrangements. Partial funding for this project has come from the General Research Fund of the University of

Kansas and through NSF-EPSCoR grant to the University of Kansas and to Kansas State University. This research has made use of the SIMBAD database, operated at CDS, Strasbourg, France.

REFERENCES

- Andersen, T. B., & Jensen, K. S. 1985, *A&AS*, 59, 361
- Anthony-Twarog, B. J. 1987, *AJ*, 93, 647
- Anthony-Twarog, B. J., Heim, E. A., Twarog, B. A., & Caldwell, N. 1991, *AJ*, 102, 1056
- Anthony-Twarog, B. J., Mukherjee, K., Caldwell, N., & Twarog, B. A. 1988, *AJ*, 95, 1453
- Anthony-Twarog, B. J., & Twarog, B. A. 1987, *AJ*, 94, 1222
- Anthony-Twarog, B. J., Twarog, B. A., & Shodhan, S. 1989, *AJ*, 98, 1634
- Balona, L. A., & Koen, C. 1994, *MNRAS*, 267, 1071
- Bertelli, G., Bressan, A., Chiosi, C., Fagotto, F., & Nasi, E. 1994, *A&AS*, 106, 275
- Carlberg, R., Dawson, P., Hsu, T., & VandenBerg, D. A. 1985, *ApJ*, 294, 674
- Carraro, G., & Chiosi, C. 1994, *A&A*, 287, 761
- Carraro, G., Ng, Y. K., & Portinari, L. 1998, *MNRAS*, 296, 1045
- Cousins, A. W. J. 1989, *South African Astron. Obs. Circ.* 13, 15
- Cousins, A. W. J. 1990, *South African Astron. Obs. Circ.* 14, 55
- Crawford, D. L. 1975, *AJ*, 80, 955
- Crawford, D. L., & Perry, C. L. 1966, *AJ*, 71, 206
- Daniel, S. A., Latham, D. W., Mathieu, R. D. & Twarog, B. A. 1994, *PASP*, 106, 281
- Eggen, O. J. 1971, *ApJ*, 166, 87 (EG)
- Edvardsson, B., Andersen, J., Gustaffson, B., Lambert, D. L., Nissen, P. E., & Tomkin, J. 1993, *A&A*, 275, 101
- Friel, E. D. 1995, *ARA&A*, 33, 381
- Grundahl, F., VandenBerg, D. A., & Andersen, M. I. 1998, *ApJ*, 500, L179
- Joner, M., & Taylor, B. 1997, *PASP*, 109, 1122
- Kilkenny, D., & Laing, J. D. 1992, *MNRAS*, 255, 308
- Kilkenny, D., & Menzies, J. W. 1986, *MNRAS*, 222, 373

- Kjeldsen, H., & Frandsen, S. 1991, A&AS, 87, 119
- Kozhurina-Platais, V., Demarque, P., Platais, I., Orosz, J. A., & Barnes, S. 1997, AJ, 113, 1045
- Marconi, G., Hamilton, D., Tosi, M., & Bragaglia, A. 1997, MNRAS, 291, 763
- Mermilliod, J. -C. 1998, WEBDA data base,
<http://obswww.unige.ch/webda/information.html>
- Mermilliod, J. -C., Andersen, J., Nordström, B., & Mayor, M. 1995, A&A, 299, 53
- Meusinger, H., Reimann, H. -G., & Stecklum, B. 1991, A&A, 245, 57
- Meynet, G., Mermilliod, J. -C., & Maeder, A. 1993, A&AS, 98, 477
- Nissen, P. E. 1988, A&A, 199, 146
- Nissen, P. E., Twarog, B. A., & Crawford, D. L. 1987, AJ, 93, 634
- Nissen, P. E., & Schuster, W. E. 1997, A&A, 326, 751
- Nordström, B., Andersen, J., & Andersen, M. I. 1996, A&AS, 118, 407
- Nordström, B., Andersen, J., & Andersen, M. I. 1997, A&A, 322, 460
- Olsen, E. H. 1983, A&AS, 54, 55
- Olsen, E. H. 1988, A&A, 189, 173
- Olsen, E. H. 1993, A&AS, 102, 89
- Perry, C. L., Franklin, C. B., Landolt, A. U., & Crawford, D. L. 1976, AJ, 81, 632
- Perry, C. L., Olsen, E. H., & Crawford, D. L. 1987, PASP, 99, 1184
- Perryman, M. A. C. *et al.* 1998, A&A, 331, 81
- Phelps, R. L., & Janes, K. A. 1994, ApJS, 90, 31
- Piatti, A. E., Claria, J. J., & Bica, E. 1998, ApJS, 116, 263
- Pols, O. R., Schröder, K. -P., Hurley, J. R., Tout, C. A., & Eggleton, P. P. 1998, MNRAS, 298, 525
- Rosvick, J. M., & Vandenberg, D. A. 1998, AJ, 115, 1516
- Schuster, W. J., & Nissen, P. E. 1988, A&AS, 73, 225
- Schuster, W. J., & Nissen, P. E. 1989, A&A, 221, 65
- Schwan, H. 1991, A&A, 243, 386
- Shobbrook, R. R. 1984, MNRAS, 206, 273
- Shobbrook, R. R. 1985, MNRAS, 212, 591

- Shobbrook, R. R. 1987, MNRAS, 225, 999
- Tosi, M., Pulone, L., Marconi, G., & Bragaglia, A. 1998, MNRAS, 299, 834
- Twarog, B. A. 1980, ApJ, 242, 242
- Twarog, B. A. 1983, ApJ, 267, 207
- Twarog, B. A. 1984, AJ, 89, 523
- Twarog, B. A., & Anthony-Twarog, B. J. 1995, AJ, 109, 2828
- Twarog, B. A., Anthony-Twarog, B. J., & Bricker, A. R. 1999, AJ, 117, 1816
- Twarog, B. A., Anthony-Twarog, B. J., & McClure, R. D. 1993, PASP, 105, 78
- Twarog, B. A., Ashman, K. M., & Anthony-Twarog, B. A. 1997, AJ, 114, 2556 (TAAT)
- Wielen, R., Fuchs, B., & Dettbarn, C. 1996, A&A, 314, 438

Fig. 1.— CMD for stars in the CCD field of IC 4651 which have at least two observations in b and y .

Fig. 2.— Photometric uncertainty in $(b - y)$ for the stars in Fig. 1 as a function of V .

Fig. 3.— Same as Fig. 1, but restricted to stars with $\sigma_{(b-y)} \leq 0.010$.

Fig. 4.— Color-color relation for stars at the cluster turnoff that have at least two observations in each filter and uncertainties in m_1 , c_1 , and $H\beta \leq 0.015$. Filled circles are stars classified as evolved while crosses are stars with anomalously high c_1 .

Fig. 5.— CMD for stars in Fig. 4. Symbols have the same meaning as in Fig. 4.

Fig. 6.— Superposition of the Hyades main sequence with the unevolved main sequence of IC 4651. The Hyades points are shifted assuming $(m - M) = 10.15$ and $E(b - y) = 0.062$. Different symbols represent the noted photometric sources.

Fig. 7.— Superposition of the unevolved main sequence of the $Z = 0.02$ isochrones of Bertelli et al. (1994) with the Hyades, assuming a Hyades modulus of 3.33.

Fig. 8.— Superposition of IC 4651 with the isochrones of Bertelli et al. (1994) adjusted for $(m - M) = 10.15$ and $E(b - y) = 0.062$.

Fig. 9.— Color-color data for the turnoff of IC 4651 superposed on the Hyades data adjusted for reddening.

Fig. 10.— Red giant clump of IC 4651. Filled circles are single stars, open circles are binaries, and starred points are stars in the field of IC 4651 for which no information is available beyond $(b - y)$.

Fig. 11.— Superposition of the CMD of NGC 3680 with that of IC 4651. Crosses are stars in IC 4651 while the starred points are identified binaries. Open circles are probable binaries in NGC 3680 while filled circles are single stars or stars for which no binary data are available. The photometry in NGC 3680 has been adjusted solely by increasing $(b - y)$ by 0.04.